ORIGINAL

Nicos Kalapodis · **Georgios Kampas** · **Olga-Joan Ktenidou**

Revisiting the fundamental structural dynamic systems: the effect of low gravity

Abstract This paper revisits the fundamental structural dynamic systems with regard to the effect of gravity, and thus self-weight, on their dynamic characteristics and response. Far from being a purely theoretical exercise, as would have been the case in the past, this study is a first step in structural dynamics inspired by—and anticipating—the potential of building under extraterrestrial conditions. More specifically, five basic structural models are considered: (a) the simple pendulum (SP), (b) the rigid inverted pendulum (RIP), (c) the flexural inverted pendulum (FIP), (d) the rigid rocking block (RRB), and (e) the flexural rocking block (FRB). The focus is to identify patterns and regions where low gravity can have a beneficial or detrimental role on the structural response. The paper initially presents the effect of low gravity on the dynamic characteristics of each system and then proceeds with highlighting their self-similar response, along with the differences in response due to low gravity. It is proved that low gravity is detrimental for the SP, while it is beneficial for the RIP and FIP models. Nevertheless, the effect can be both beneficial and detrimental for the RRB and FRB, depending on their parameters as revealed from this investigation. Finally, the main dynamic characteristics of the five cases studied, factorized by the gravitational multiplier (α), are quantified and summarized in the form of a representative table.

1 Introduction and background

In an effort to simulate the behavior of different types of structures under dynamic excitations, many studies in the past have developed different fundamental structural dynamic models. The simplest and most fundamental model is the single-degree-of-freedom (SDOF) system that consists of a mass connected to a spring and a dashpot (Chopra [1], Clough and Penzien [2] among others). The beneficial role of the spring is due to the restoring forces from the structural elements that provide a positive stiffness and allows the system to vibrate during and after the excitation. However, several decades ago and especially after the 1995 Kobe earthquake, it was obvious that the conventional structural design should adopt a more holistic view of the structure,

N. Kalapodis (✉)
Department of Civil Engineering, University of Patras, 26504 Rio, Patras, Greece
E-mail: nkalapodis@upatras.gr
Tel.: +30-6974131490

G. Kampas
School of Engineering, University of Greenwich, Central Avenue, Chatham ME4 4TB, UK

O.-J. Ktenidou
Institute of Geodynamics, National Observatory of Athens, Lofos Nymphon - Thissio, 11851 Athens, Greece

including the superstructure, foundation and the soil (soil–structure interaction, SSI) [3–6]. Therefore, there was a transition from the SDOF cantilever systems to inverted pendulum-like models since the fixity at the base was replaced by a rotational spring accounting for the SSI. Thus, for structures where either the dissipation of energy takes place mainly at the base of a single building element or the main mass (over than 50%) is in the upper third of its height, the dynamic system can be considered as an inverted pendulum [7]. [8] and Housner [9] were pioneers in introducing structures that exhibited an inverted pendulum-like behavior, characterized later on as rocking behavior. The transition from inverted pendulum to rocking systems occurs with the addition of the element's width (thus introducing slenderness) and the differentiation of pivot points at each rocking cycle. This paper focuses on the clear distinction between the aforementioned models and elucidate their dynamic responses' differences when moving from positive (inverted pendulum) to negative stiffness systems (rocking).

There is considerable ongoing research on rocking structures, whether for the purpose of investigating the seismic resilience of ancient monuments such as ancient temples or arches [10–13] or as an alternative technique for seismic isolation, in order to decrease the forces transferred to the foundation [13–17]. However, the observation of large, slender elements (wind-turbines, industrial chimneys, piers in valley bridges, etc.) that exhibit rocking behavior led to the coupling of flexural vibrations with rocking response, and therefore introduced the so-called flexural rocking models [18–22]. Nevertheless, the role of self-weight on the dynamic response of the different systems has not been thoroughly investigated until now, with the exception of the second-order ($P - \Delta$) effects in flexible cantilever systems [23,24]. The objective of this study is to investigate the role of weight on the dynamic characteristics and on the response of the different fundamental structural dynamic systems pertaining to civil engineering structures; fundamental dynamic systems exhibiting chaotic behavior (such as the Duffing oscillator) that can be of interest from a mechanical engineering perspective are not included in this study.

The motivation behind this objective is not merely academic but stems mostly from the enormous streamline of investments from various industrial firms and federal agencies (NASA, SpaceX, Boeing, Virgin Galactic, ESA, etc.) to expand civil engineering in extraterrestrial conditions, be it for the development of Lunar and Martian outposts or for Space tourism. Although some preliminary steps toward the conceptualization of extraterrestrial structures have already been made [25–30], the effect of low gravity on a wide range of structures (with or without the consideration of foundations/SSI) is not yet fully understood.

Hence, to take the first step in this direction, this paper revisits the fundamental structural dynamic systems and focuses on the effect of low gravity on their dynamic characteristics and thus on their dynamic structural response. The five systems considered herein are: (a) the simple pendulum (SP), (b) the rigid inverted pendulum (RIP), (c) the flexural inverted pendulum (FIP), (d) the rigid rocking block (RRB), and (e) the flexural rocking block (FRB), all of which are subjected to a simple harmonic excitation. The excitation was chosen as a single-cycle sine pulse, as this is the simplest waveform that can be identified as a 'dangerous' component of strong ground motion for structures [13]. The parameterization used is designed to reveal any self-similar response and to identify critical combinations of parameters where low gravity becomes dominant (beneficially or detrimentally) for structural behavior.

2 Fundamental structural dynamic systems

As mentioned above, the present work focuses on the effect of low gravity on the dynamic characteristics and response of five fundamental structural dynamic systems, subjected to a single harmonic pulse. In what follows, one subsection is dedicated to each system: First, each system is described with the aim to reveal its geometric and dynamic characteristics as a function of gravity, and then the study reveals any existing self-similarity, focusing on the effect of low gravity for different values of gravitational acceleration (αg). The values of the gravitational multiplier, α, considered in this study are set equal to 0.17, 0.38 and 1.00, as reference values for the cases of the Moon, Mars and Earth respectively. Note that damping was not considered in any of the models except FRB, because: (a) the aim is to highlight the effect of low gravity, and (b) there is not enough evidence as to how low gravity can affect damping.

2.1 Simple pendulum (SP)

At first, the most fundamental dynamic system, the simple pendulum, is investigated herein, where a concentrated mass (m) is suspended from a pivot point via a massless thread, so that it can swing freely (Fig. 1a).
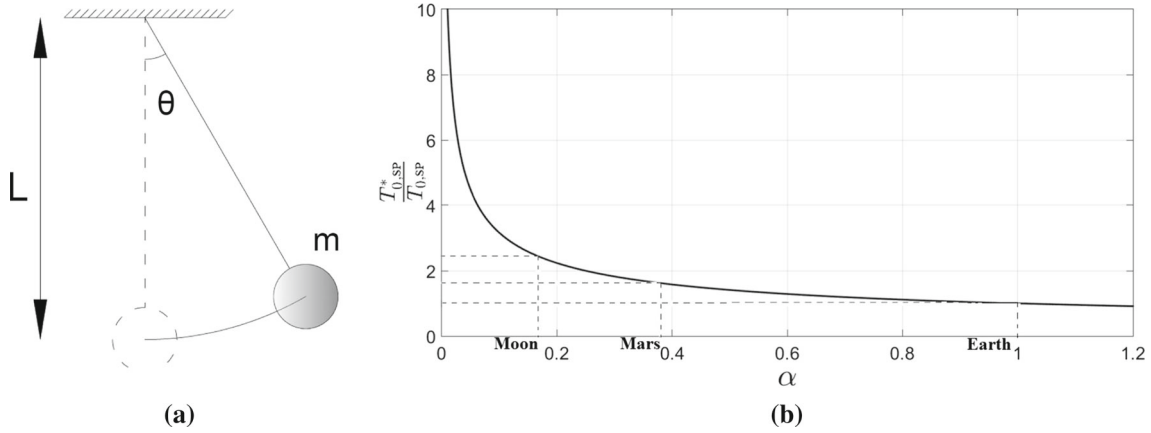
Fig. 1 a Simple harmonic pendulum; **b** the influence of the gravitational acceleration α to the natural period of the system by assuming zero damping

Although this system usually does not explicitly represent structural behavior, except some specific applications (tuned mass damper, friction pendulum bearing, etc.), it aims to serve as a reference case to illustrate critical aspects of the effect of low gravity on its behavior. More specifically, gravity plays a stabilizing role here, since it creates a restoring force that compels the mass to oscillate about the equilibrium point. By assuming zero damping, the motion of the concentrated mass subjected to a linear sinusoidal excitation, can be described by Eq. (1) as:

$$\ddot{\theta} + \frac{ag}{L}\sin(\theta) = \frac{A_p}{L}\sin\left(\frac{2\pi}{T_P}t\right) \overset{\sin\theta \approx \theta}{\Longrightarrow} \ddot{\theta} + \frac{ag}{L}\theta = \frac{A_p}{L}\sin\left(\frac{2\pi}{T_P}t\right) \tag{1}$$

where g, L, α are the reference acceleration of gravity in earth, the length of the thread, and the gravitational multiplier, respectively. $\ddot{\theta}$ and θ are the rotational acceleration and chord rotation considered at the pivot point. A_p, T_p are the amplitude and the pulse period of the linear excitation respectively. The maximum values of total displacements ($u_{\max}$) and rotations ($\theta_{\max}$) usually exhibited by civil engineering systems are very small compared to the geometry of the structure and thus, the linearized equations of motions $\theta \approx 0$, $\sin\theta \approx \theta$, $\cos\theta \approx 1$) are used herein to describe the dynamic response of the systems.

The exact expression of the natural period of a simple pendulum $\left(\hat{T}_{0,\mathrm{SP}}^{*}\right)$ along with the corresponding expression of the natural period obtained by a small-angle approximation $\left(T_{0,\mathrm{SP}}^{*}\right)$, are defined as follows:

$$\hat{T}_{0,\mathrm{SP}}^{*} = 2\pi\sqrt{\frac{L}{\alpha g}} \cdot \sum_{n=0}^{\infty}\left(\left(\frac{(2n)!}{(2^n \cdot n!)^2}\right)^2 \cdot \sin^{2n}\frac{\theta}{2}\right) \overset{\theta \approx 0}{\Longrightarrow} T_{0,\mathrm{SP}}^{*} = 2\pi\sqrt{\frac{L}{\alpha g}} = \frac{1}{\sqrt{\alpha}}T_{0,\mathrm{SP}} \tag{2}$$

The effect of the gravitational multiplier, (α), on the natural period of the harmonic pendulum is shown in Fig. 1b for the three distinct reference values of α (0.17, 0.38 and 1.00). $T_{0,\mathrm{SP}}$ corresponds to the natural period of a simple pendulum under the assumption that $\alpha = 1.00$. Figure 1b shows how dominant low gravity (i.e., low values of α) can become, as it increases the natural period of the SP significantly and with a geometric rate. The response of the system is a function of five variables: $\theta = f\left(L, g, \alpha, T_p, A_p\right)$, involving two fundamental dimensions. According to Buckingham's theorem [31], the response can be described by $6 - 2 = 4$ dimensionless parameters, which are shown below:

$$\Pi_\theta = \theta, \quad \Pi_\alpha = \alpha, \quad \Pi_g = \frac{A_p}{g}, \quad \Pi_{T_{\mathrm{SP}}} = \frac{T_{0,\mathrm{SP}}}{T_p} \tag{3}$$

Thus, the response of the system is fully described by:

$$\theta = \varphi\left(\alpha, \frac{A_p}{g}, \frac{T_{0,\mathrm{SP}}}{T_p}\right) \tag{4}$$

The self-similar response of the system, $\frac{\Pi_\theta \Pi_\alpha}{4\pi^2 \Pi_g}$, when subjected to a single sinusoidal pulse can be deduced from the dimensionless master curve presented in Fig. 2a, which was computed by means of a small-angle approximation and for a wide range of values of $\frac{\Pi_{T_{SP}}}{\sqrt{\Pi_\alpha}} = T_{0,SP}^*/T_p$.

On the other hand, Fig 2b shows the dimensionless response, $\frac{\Pi_{\theta \max}}{4\pi^2 \Pi_g}$, of the nonlinear SP system against the "nonlinear" dimensionless period ratio, $\hat{T}_{0,SP}^*/T_p$, subjected to one-pulse sinusoidal excitations. θ_0 is defined as the max $\left\{ \max |\theta| \text{ for a certain } \hat{T}_{0,SP}^*/T_p \right\}$. The influence of large angles is illustrated in Fig. 2b, where higher discrepancy between the small-angle approximation (Fig. 2a—master curve) and the exact nonlinear response is observed for higher response angles due to either the effect of low gravity (e.g., for $\alpha = 0.17$), or due to higher excitation amplitudes; both these factors result to higher dimensionless response values, $\frac{\Pi_{\theta \max}}{4\pi^2 \Pi_g}$.

Given the self-similar response and the master curve of Fig. 2a, the low-gravity effect can be illustrated when the dimensional response, $\frac{\Pi_{\theta \max}}{4\pi^2 \Pi_g}$, is presented against the dimensionless period $\Pi_{T_{SP}}$ for the three distinct values of the gravitational multiplier, Π_α. Therefore, Fig 3 depicts dimensionless response spectra curves for the cases of $\alpha = 0.17, 0.38$ and 1.00. The purpose of this figure is to illustrate the response of different SPs with known values of natural periods on Earth ($T_{0,SP}$) when subjected to given harmonic excitations (T_p) at different gravitational fields (α). By observing Fig. 3, it is evident that lower values of gravity, α, lead to higher dimensionless response values $\frac{\Pi_{\theta \max}}{4\pi^2 \Pi_g}$ and the resonance intervals shift toward smaller $\Pi_{T_{SP}}$ values.
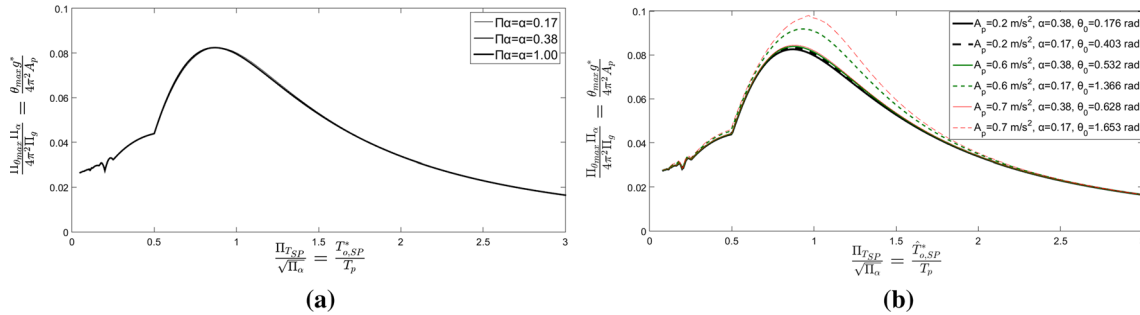
Fig. 2 a Dimensionless response spectrum of an SP subjected to a one-cycle sinusoidal pulse, exhibiting self-similar behavior for a large range of dimensionless periods, $T_{0,SP}^*/T_p$, obtained by considering a small-angle approximation; **b** the influence of the angular response in the dimensionless response spectrum of an SP, subjected to a one-cycle sinusoidal pulse
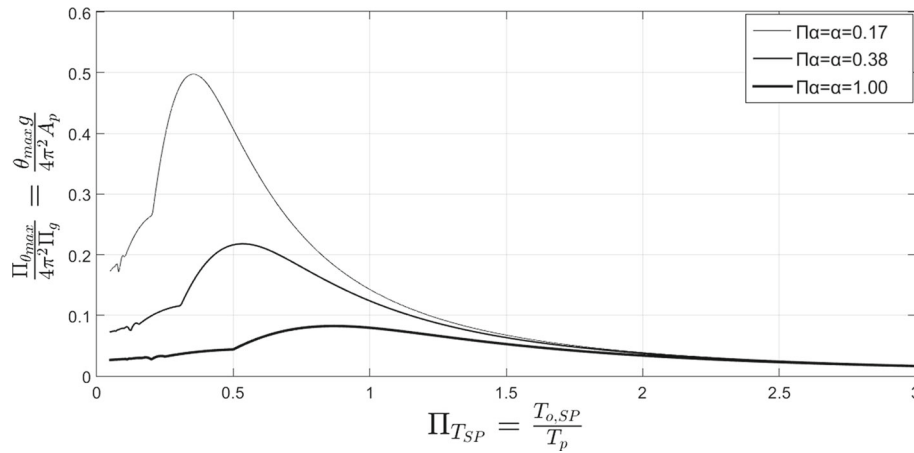
Fig. 3 Dimensionless response spectra of the SP, $\frac{\Pi_{\theta \max}}{4\pi^2 \Pi_g}$, against the dimensionless reference period, $\Pi_{T_{SP}}$, for the three distinct values of the gravitational multiplier, Π_α, when subjected to a single sinusoidal pulse

2.2 Rigid inverted pendulum (RIP)

A rigid inverted pendulum is defined as a concentrated mass which is connected with a rotational spring having a finite rotational stiffness equal to K_r (Fig. 4a) through a rigid linear bar.

Contrary to SP, for the case of rigid inverted pendulum, the gravity plays a destabilizing role, while the rotational stiffness of the spring prevents the system from acting like a mechanism. By observing the equation of motion:

$$\ddot{\theta} + \frac{K_r}{mL^2}\theta - \frac{ag}{L}\sin\theta = \frac{A}{L}\sin\left(\frac{2\pi}{T_P}t\right) \overset{\sin\theta \approx \theta}{\Longrightarrow} \ddot{\theta} + \left(\frac{K_r}{mL^2} - \frac{ag}{L}\right)\theta = \frac{A}{L}\sin\left(\frac{2\pi}{T_P}t\right), \quad (5)$$

one can conclude that the gravitational force (self-weight) reduces the overall stiffness of the system. Furthermore, the physical constraint (positive stiffness), $\left(\frac{K_r}{mL^2} - \frac{ag}{L}\right) > 0$, allowing the system to vibrate, results in strictly $\alpha < \alpha_{cr}$, with $\alpha_{cr} = \frac{K_r}{mgL}$.

Figure 4b indicates that a decreasing value of α/α_{cr} (that has to be less than unity), leads also to decrease in the natural period of the system as:

$$T^*_{0,RIP} = 2\pi\sqrt{\frac{mL^2}{K_r - m\alpha gL}} = 2\pi\frac{1}{\sqrt{\frac{K_r}{mL^2} - \alpha\frac{g}{L}}} = \frac{1}{\sqrt{\alpha_{cr} - \alpha}}T_{0,SP} \quad (6)$$

From Eqs. (2) and (6), it is evident that RIP becomes a stiffer configuration with lower gravity, compared to the SP that becomes more flexible.

The response of the RIP is a function of seven parameters $\theta = f\left(m, K_r, L, g, \alpha, T_p, A_p\right)$ with three reference dimensions, and therefore by applying Buckingham's theorem, we need $8 - 3 = 5$ dimensionless parameters. The five dimensionless parameters that can fully describe the response of the system are:
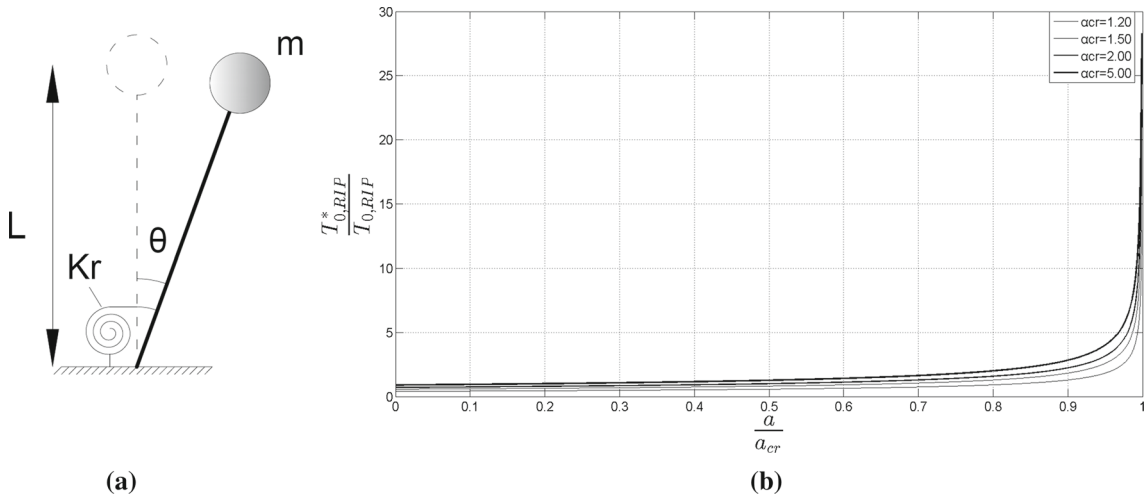
$$\Pi_\theta = \theta, \quad \Pi_\alpha = \alpha, \quad \Pi_g = \frac{A_p}{g}, \quad \Pi_{T_{RIP}} = \frac{T_{0,RIP}}{T_p}, \quad \Pi_{\alpha_{cr}} = \alpha_{cr} \quad (7)$$

Thus, the response of the system is fully described by:

$$\theta = \varphi\left(\alpha, \frac{A_p}{g}, \frac{T_{0,RIP}}{T_p}, \alpha_{cr}\right) \quad (8)$$

or by a combination of these.

The response of a RIP in terms of rotation (θ) and rotational velocity ($\dot{\theta}$) of the base, is shown in Fig. 5 for gravitational multiplier $\Pi_\alpha = \alpha = \{0.17, 0.38, 1.00\}$ and $\Pi_{\alpha_{cr}} = \alpha_{cr} = 1.5$.

| (a) | (b) |

Fig. 4 a Rigid inverted pendulum (RIP); **b** the influence of the gravitational multiplier α on the natural period of the system
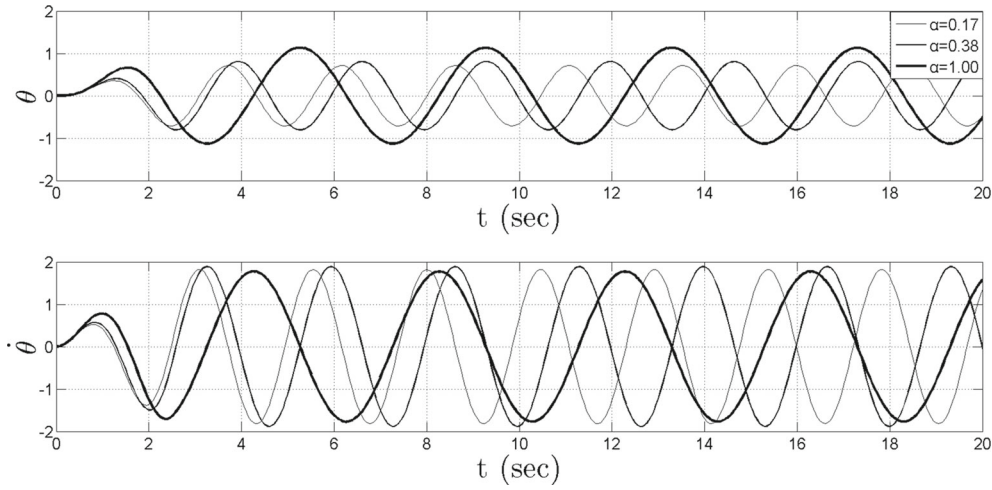
Fig. 5 Time history of a RIP subjected to a single sinusoidal impulse of $\Pi_g = 0.3$ and $T_p = 2.5\,\mathrm{s}$, where $T_{0,\mathrm{RIP}} = 4.0\,\mathrm{s}$, $\Pi_\alpha = \{0.17, 0.38, 1.00\}$ and $\Pi_{\alpha_{\mathrm{cr}}} = 1.5$
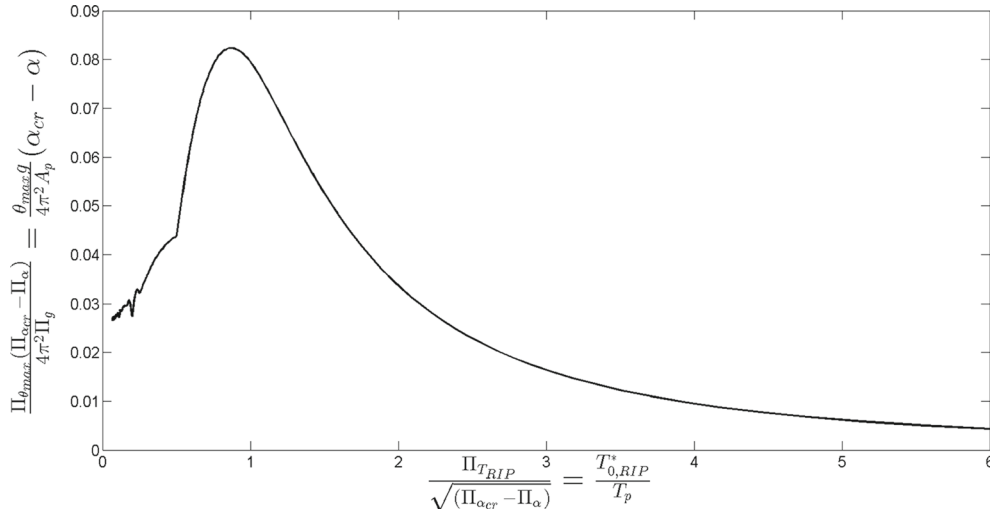

Fig. 6 Self-similar master curve concerning the dimensionless response spectrum of the RIP against a large range of $T_{0,\mathrm{RIP}}^*/T_p$ subjected to one-cycle sinusoidal pulse

Similarly to the SP case, a self-similar master curve is revealed in Fig. 6 when the dimensionless response, $\frac{\Pi_\theta(\Pi_{\alpha_{\mathrm{cr}}}-\Pi_\alpha)}{4\pi^2\Pi_g}$, is presented against a wide range of dimensionless period, $\frac{\Pi_{T_{\mathrm{RIP}}}}{\sqrt{(\Pi_{\alpha_{\mathrm{cr}}}-\Pi_\alpha)}} = T_{0,\mathrm{RIP}}^*/T_p$. It is worth noting that the difference between the two systems is the substitution of $\Pi_{\alpha,(\mathrm{SP})}$ with $\Pi_{\alpha_{\mathrm{cr}}} - \Pi_{\alpha,(\mathrm{RIP})}$ which clearly indicates the reversal of the role of gravity (from stabilizing to destabilizing).

For a structure that can be modeled as a RIP (water towers, silos, etc.), *the* $\alpha_{\mathrm{cr}} = \Pi_{\alpha_{\mathrm{cr}}} = \frac{K_{\mathrm{r}}}{mgL}$ factor is indicative of how rotationally stiff the foundation is (soil–structure interaction), relative to how susceptible the system is to overturn by its own weight ($P - \Delta$ effect $= mgL\theta$). Therefore, high values of α_{cr} mean that the rotational stiffness (K_{r}) of the system is substantially increased and hence does not permit the development of large base rotation (θ), despite the mass (m) and height (L) of the structure.

The influence of low gravity on the response of the RIP to a single sine pulse can be revealed if the dimensionless response, $\frac{\Pi_{\theta_{\max}}}{4\pi^2\Pi_g}$, is presented against the reference dimensionless period $\Pi_{T_{\mathrm{RIP}}}$, for distinct values of the gravitational multiplier, Π_α and for different $\Pi_{\alpha_{\mathrm{cr}}}$ values (Fig. 7). It is evident that for RIPs of the same α_{cr}, lower values of α lead to smaller rotations at the base ($\theta_{\max}$), as the destabilizing factor of gravity decreases. However, for higher values of α_{cr}, the response of the system appears to be substantially lower, since the rotational spring is stiffer and thus the effect of low gravity as α_{cr} increases becomes negligible.
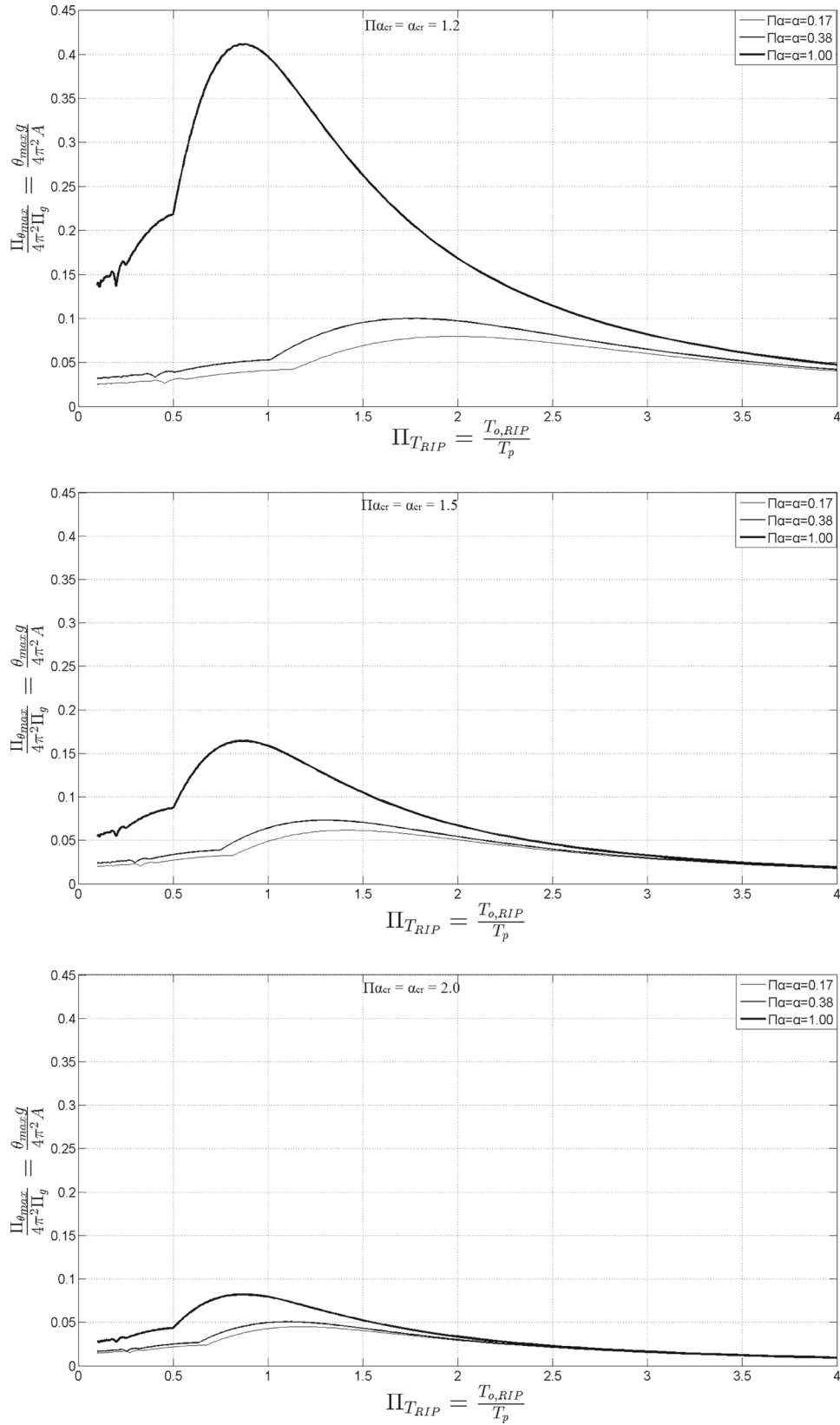
Fig. 7 Dimensionless response spectra of the RIP when subjected to a single sinusoidal pulse with period T_p and amplitude A_p, for different values of α and α_{cr}

2.3 Flexural inverted pendulum (FIP)

A more realistic approach regarding the modeling of structures that behave in an inverted pendulum-like way is presented in this subsection. The FIP (Fig. 8) retains the characteristics of a RIP, the difference being that the concentrated mass at the top is connected with the rotational spring through a flexural linear member. Thus, the FIP is a dynamic system of two degrees of freedom (θ, u), but without a mass assigned to each degree. Hence, the system of Fig. 8 is described as a pseudo-single-degree-of-freedom (SDOF) system and not as a two-degree-of-freedom system. However, adopting a Lagrangian formulation (see "Appendix"), the equations of motion [Eqs. (9) and (10)] can be obtained:

$$\begin{aligned} mL\cos(\theta)\ddot{u}_g &+ mL^2\ddot{\theta} + 2mu\dot{u}\dot{\theta} + mu^2\ddot{\theta} + mL\ddot{u} + K_\mathrm{r}\theta \\ &-m\alpha g L\sin(\theta) - m\alpha g u\cos(\theta) = mu\sin(\theta)\ddot{u}_g \end{aligned} \tag{9}$$

$$m\ddot{u} + mL\ddot{\theta} - mu\dot{\theta}^2 + ku - m\alpha g\sin(\theta) = m\cos(\theta)\ddot{u}_g \tag{10}$$

Structures in real life possess a finite stiffness and can exhibit large lateral displacements in extreme circumstances, such as strong wind loads or ground motions. Those lateral displacements, combined with high vertical loads (usually related to gravity loads), are responsible for the development of second-order effects [23,24] which constitute an additional load for the structure. Such a phenomenon creates a destabilizing moment equal to the vertical force multiplied by the horizontal structural displacement when loaded laterally. In order to take the $P - \Delta$ effect under consideration, the stiffness of the flexural member is set to: $k = 3\frac{EI}{L^3} - \frac{\alpha m g}{L}$ (where $k_\mathrm{cant} = 3\frac{EI}{L^3}$ is defined as the cantilever stiffness). The response of the flexural inverted pendulum is a function of eight parameters $\theta = f(m, k, K_\mathrm{r}, L, g, \alpha, T_p, A_p)$ with three reference dimensions, therefore: $9 - 3 = 6$. The six dimensionless parameters that can fully describe the response of the system are:

$$\Pi_\theta = \theta_\mathrm{tot} = \frac{u_{tot}}{L} = \left(\theta + \frac{u}{L}\right)$$

$$\Pi_\alpha = \alpha; \quad \Pi_g = \frac{A_p}{g}; \quad \Pi_{T_\mathrm{FIP}} = \frac{T_{0,\mathrm{FIP}}}{T_p}; \quad \Pi_{\alpha_\mathrm{cr}} = \alpha_\mathrm{cr}$$

$$\Pi_k = \frac{kL^2}{K_\mathrm{r}} \quad \text{(without } p - \Delta\text{)}; \quad \Pi_{k_\mathrm{cant}} = \frac{k_\mathrm{cant}L^2}{K_\mathrm{r}} \quad \text{(including } p - \Delta\text{)} \tag{11}$$

Thus, the total horizontal response of the system is fully described by:

$$\theta_\mathrm{tot} = \varphi\left(\alpha, \ \frac{A_p}{g}, \ \frac{T_{0,\mathrm{FIP}}}{T_p}, \alpha_\mathrm{cr}, \frac{k_\mathrm{cant}L^2}{K_\mathrm{r}}\right) \tag{12}$$

or by a combination of these.
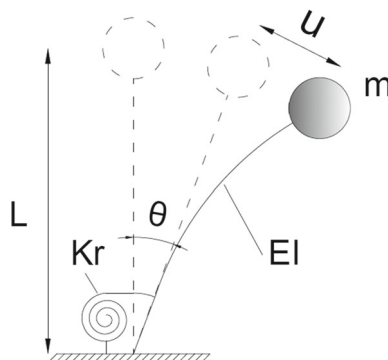
Fig. 8 Flexural inverted pendulum system

Since the FIP of Fig. 8 is a pseudo-SDOF (as one rather than two masses exist), only one natural period can be extracted from the linearized equations of motion [Eqs. (9) and (10)]:

$$T^*_{0,\text{FIP}} = 2\pi \sqrt{\frac{K_{\text{r}}m + mL^2k + m^2\alpha g L}{K_{\text{r}}k - m\alpha g L k - m^2\alpha^2 g^2}} = \sqrt{\frac{1 + \frac{\alpha}{\alpha_{\text{cr}}} + \Pi_k}{\alpha_{\text{cr}}\left[\Pi_k - \Pi_k\frac{\alpha}{\alpha_{\text{cr}}} - \left(\frac{\alpha}{\alpha_{\text{cr}}}\right)^2\right]}} \, T_{0,\text{SP}} \tag{13}$$

From the natural period of the system, a physical constrain arises similarly to the previous systems; the maximum value of the gravitational multiplier (α) should be between $0 < \alpha \le \frac{k}{2mg}\left(\sqrt{L^2 + 4\frac{K_{\text{r}}}{k}} - L\right)$. The aforementioned upper limit of (α) factor is symbolized as α'_{cr} in order to avoid being confused with the corresponding α_{cr} which is relevant to RIP. The expression of α'_{cr} is described by the Eqs. (14) and (15), and it is also correlated with the dimensionless stiffness parameter Π_k.

$$\alpha'_{\text{cr}} = \frac{K_{\text{r}}}{mgL}\left(\sqrt{\left(\frac{kL^2}{2K_{\text{r}}}\right)^2 + \frac{kL^2}{K_{\text{r}}}} - \frac{kL^2}{2K_{\text{r}}}\right) = \Pi_{\alpha_{\text{cr}}}\left(\sqrt{\left(\frac{\Pi_k}{2}\right)^2 + \Pi_k} - \frac{\Pi_k}{2}\right) \tag{14}$$

Interestingly, the FIP has two independent limiting cases; firstly, when $K_{\text{r}} \to \infty$, the system becomes a vertical cantilever and on the other hand, when $k \to \infty$, then the structure resembles a RIP. The aforementioned conclusion can be proved as follows:

$$\lim_{K_{\text{r}}\to\infty} \omega^2_{\text{FIP}} = \lim_{K_{\text{r}}\to\infty}\left(\frac{K_{\text{r}}k - m\alpha g L k - m^2\alpha^2 g^2}{K_{\text{r}}m + mL^2k + m^2\alpha g L}\right) = \lim_{K_{\text{r}}\to\infty}\left(\frac{\frac{K_{\text{r}}k}{K_{\text{r}}} - \frac{m\alpha g L k}{K_{\text{r}}} - \frac{m^2\alpha^2 g^2}{K_{\text{r}}}}{\frac{K_{\text{r}}m}{K_{\text{r}}} + \frac{mL^2k}{K_{\text{r}}} + \frac{m^2\alpha g L}{K_{\text{r}}}}\right)$$

$$= \frac{k}{m} = \omega^2_k \quad \text{and} \quad \Pi_k \to 0$$

$$\lim_{k\to\infty} \omega^2_{\text{FIP}} = \lim_{k\to\infty}\left(\frac{K_{\text{r}}k - m\alpha g L k - m^2\alpha^2 g^2}{K_{\text{r}}m + mL^2k + m^2\alpha g L}\right) = \lim_{k\to\infty}\left(\frac{\frac{K_{\text{r}}k}{k} - \frac{m\alpha g L k}{k} - \frac{m^2\alpha^2 g^2}{k}}{\frac{K_{\text{r}}m}{k} + \frac{mL^2k}{k} + \frac{m^2\alpha g L}{k}}\right)$$

$$= \frac{K_{\text{r}} - magL}{mL^2} = \omega^2_{\text{RIP}} \quad \text{and} \quad \Pi_k \to +\infty$$

By considering $p - \Delta$ effects and substituting k with $k_{\text{cant}} - \frac{\alpha mg}{L}$ in Eq. (13), we reach Eqs. (15) and (16)

$$T^*_{0,\text{FIP}} = 2\pi\sqrt{\frac{K_{\text{r}}m + mL^2k + m^2\alpha g L}{K_{\text{r}}k - m\alpha g L k - \frac{K_{\text{r}}\alpha mg}{L}}} = \sqrt{\frac{1 + \Pi_{k_{\text{cant}}}}{\alpha_{\text{cr}}\left[\Pi_{k_{\text{cant}}} - \Pi_{k_{\text{cant}}}\frac{\alpha}{\alpha_{\text{cr}}} - \frac{\alpha}{\alpha_{\text{cr}}}\right]}} \, T_{0,\text{SP}} \tag{15}$$

$$\alpha'_{\text{cr}} = \frac{K_{\text{r}}}{mgL}\left(\frac{k_{\text{cant}}L^2}{K_{\text{r}} + k_{\text{cant}}L^2}\right) = a_{\text{cr}}\left(\frac{k_6 L^2}{K_{\text{r}} + k_{\text{cant}}L^2}\right) = \Pi_{\alpha_{\text{cr}}}\left(\frac{\Pi_{k_{\text{cant}}}}{1 + \Pi_{k_{\text{cant}}}}\right) \tag{16}$$

A typical time history of a FIP for gravitational multiplier $= \Pi_\alpha = \{0.17, 0.38, 1.00\}$, $\alpha_{\text{cr}} = \Pi_{\alpha_{\text{cr}}} = 3.0$ and $\Pi_k = 2.0$ is presented in Fig. 9.

In this case, the system exhibits a self-similar behavior along the full range of parameters as the previous systems. Figure 10a shows the dimensionless response, $\frac{\Pi_\theta(\alpha'_{\text{cr}} - \Pi_\alpha)}{4\pi^2\Pi_g}$, of the FIP against a wide range of $\sqrt{\frac{1 + \Pi_{k_{\text{cant}}}}{\Pi_{\alpha_{\text{cr}}}[\Pi_{k_{\text{cant}}} - \Pi_{k_{\text{cant}}}\frac{\Pi_\alpha}{\Pi_{\alpha_{\text{cr}}}} - \frac{\Pi_\alpha}{\Pi_{\alpha_{\text{cr}}}}]}} T_{0,SP}/T_p = T^*_{0,\text{FIP}}/T_p$ and $\Pi_{k_{\text{cant}}}$, when subjected to a continuous sine pulse with amplitude, A_p, and period, T_p and Fig. 10b shows the self-similar curve of a FIP subjected to one cycle sinusoidal pulse and resembles this of the RIP. Figure 10 makes a very important point for this study, as it interconnects directly the response of two seemingly different systems (RIP and cantilever) to a single master response. Obviously, the link between the two different systems is the FIP, given that the two systems are two different aspects (limit cases) of the same system (FIP).
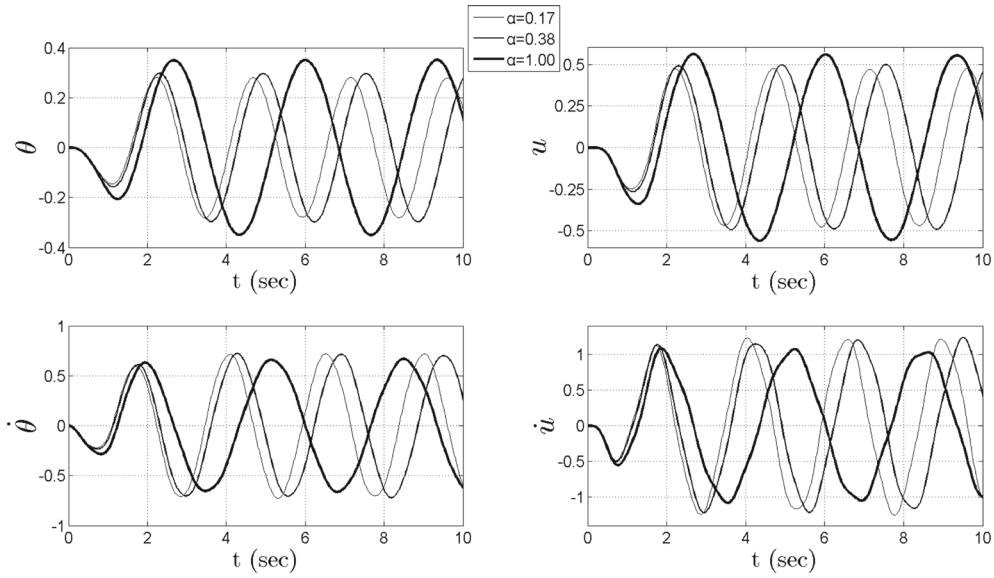
Fig. 9 Time history of a FIP subjected to a sinusoidal impulse of $\Pi_g = 0.3$ and $T_p = 2\,\text{s}$, where $T_{0,\text{SP}} = 3.47\,\text{s}$, $\Pi_\alpha = \{0.17, 0.38, 1.00\}$, $\Pi_{\alpha_{\text{cr}}} = 3.0$ and $\Pi_k = 2.0$
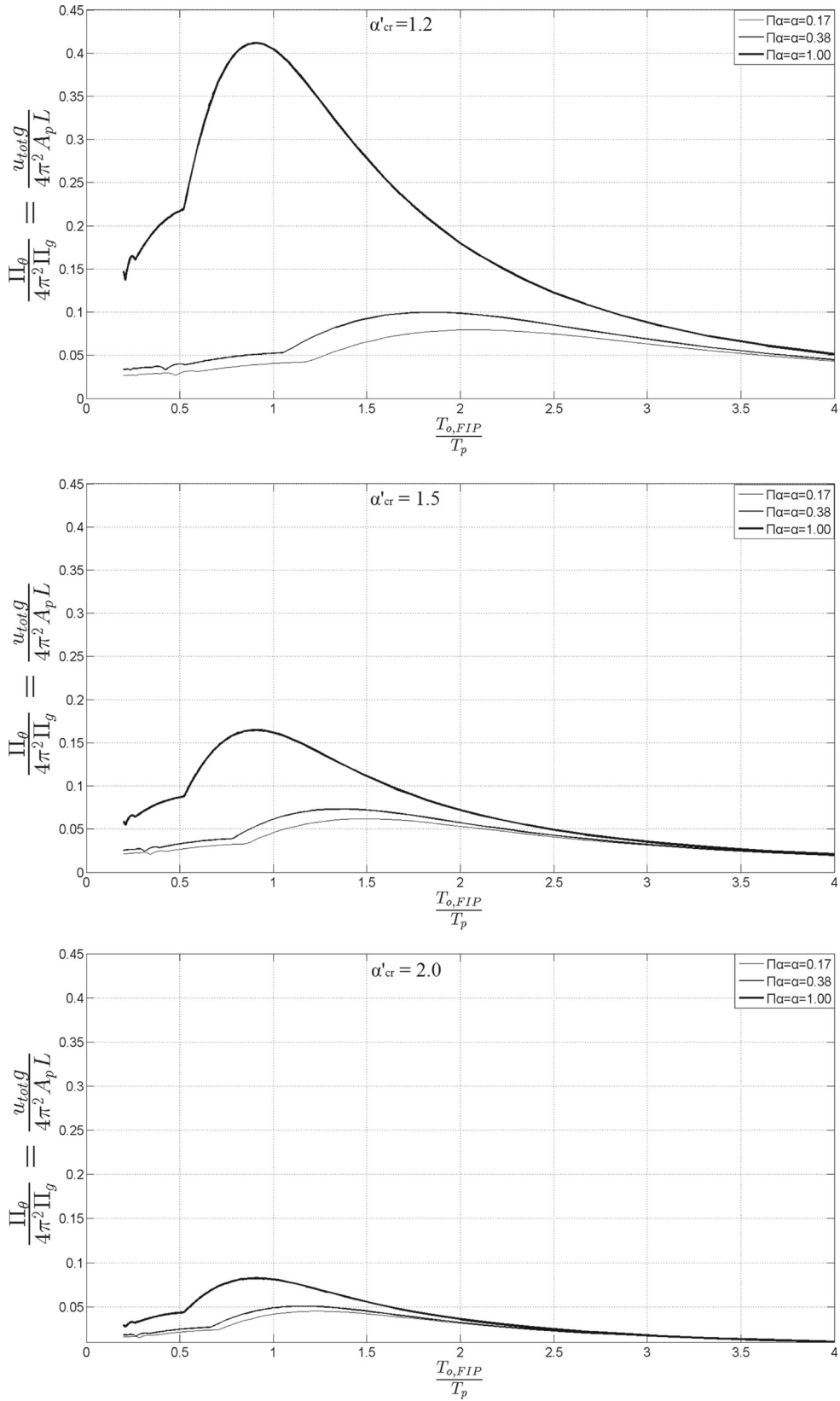

(a)   **(b)**
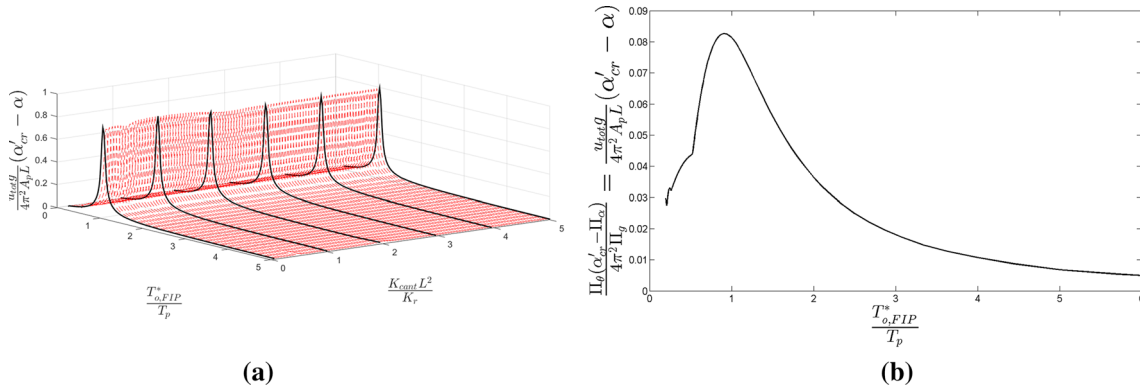
Fig. 10 a *3D* Dimensionless self-similar response spectrum of the FIP when subjected to a continuous sine pulse with period T_p and amplitude A_p, **b** self-similar spectrum curve of a FIP which is subjected to one-cycle sinusoidal pulse with period T_p and amplitude A_p

Figure 11 shows the dimensionless response of a FIP. More specifically, it depicts $\frac{\Pi_\theta}{4\pi^2\Pi_g}$, against

$$\sqrt{\frac{1+\Pi_{k_{\text{cant}}}}{\Pi_{\alpha_{\text{cr}}}[\Pi_{k_{\text{cant}}} - \Pi_{k_{\text{cant}}}\frac{1}{\Pi_{\alpha_{\text{cr}}}} - \frac{1}{\Pi_{\alpha_{\text{cr}}}}]}} T_{0,SP}/T_p = T_{0,\text{FIP}}/T_p,$$

for the three values of $\Pi_\alpha = \{0.17, 0.38, 1.00\}$ and for different values of $\alpha'_{\text{cr}} = \{1.2, 1.5, 2.0\}$. As expected, the response decreases with low gravity in a similar manner as RIP.

2.4 Rigid rocking block (RRB)

Over the past few decades, various researchers investigated the concept of a freestanding rocking rigid block resting on a rigid surface. Rocking systems are classified as a different class of systems than RIP and FIP systems, since gravity tends to restore their equilibrium—under the condition that the rotation angle (θ) defined at the pivot points (Fig. 12) will not surpass a certain threshold defined by the capacity of each block (overturning event). The equation of motion is then [9,10,22]:

$$\ddot{\theta} = -p^2\left[\sin\left(sign\left(\theta\right)a_{\text{sl}} - \theta\right) + \cos\left(sign\left(\theta\right)a_{\text{sl}} - \theta\right)\frac{\ddot{u}_g}{\alpha g}\right] \tag{17}$$

Fig. 11 Dimensionless response spectra of the flexural inverted pendulum FIP when subjected to a sine pulse with period T_p and amplitude A_p, for different values of α and α'_{cr}
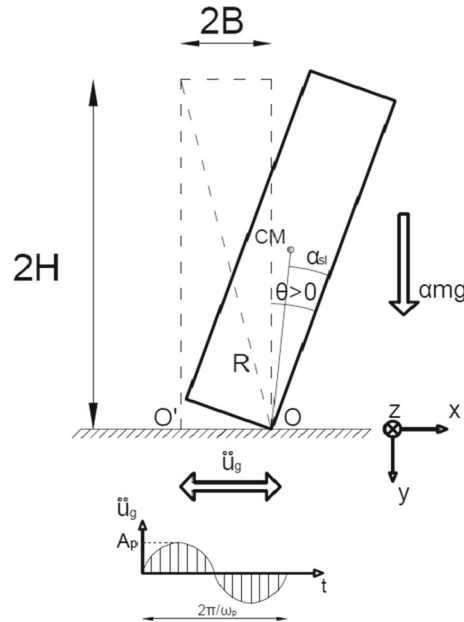
Fig. 12 Rocking of a rigid block

where $p_{\mathrm{RB}}^{*} = \sqrt{\frac{3\alpha g}{4R}}$: frequency parameter of the rigid block (RB) (rad/s) and $R = \sqrt{B^2 + H^2}$

$$a_{\mathrm{sl}} = a \tan\left(\frac{B}{H}\right) : \text{Defines the slenderness of the block}$$

The uplifting acceleration of the RB is equal to $\alpha g \tan(a_{\mathrm{sl}})$. Obviously, low gravity results in easier uplifting of the RRB. During the rocking motion, just before and after the impact, the rotation angle (θ) is equal to zero as is the potential energy of the system. Thus, the total energy of the system can be expressed in the form of kinetic energy. The energy loss according to Housner [9] is expressed by:

$$l = 1 - \left(\frac{\dot{\theta}_2}{\dot{\theta}_1}\right)^2 \tag{18}$$

The rocking response of the rigid block is a function of six parameters $\theta = f\left(\alpha_{\mathrm{sl}}, p, g, \alpha, \omega_p, A_p\right)$ with two reference dimensions, therefore by applying Buckingham's theorem: $7 - 2 = 5$. The five dimensionless parameters that can fully describe the response of the system are chosen as:

$$\Pi_\theta = \theta, \quad \Pi_{\alpha_{\mathrm{sl}}} = \tan(\alpha_{\mathrm{sl}}), \quad \Pi_\alpha = \alpha, \quad \Pi_g = \frac{A_p}{g}, \quad \Pi_\omega = \frac{\omega_p}{p} \tag{19}$$

Thus, the response of the system is fully described by:

$$\theta = \varphi\left(\alpha, \frac{A_p}{g}, \frac{\omega_p}{p}, \tan(\alpha_{\mathrm{sl}})\right) \tag{20}$$

or by a combination of these.

Figure 13 presents the rocking response time histories of a RB with $R = 7.21$ and $\alpha_{\mathrm{sl}} = 1/4$ when subjected to a one-cycle sine pulse with period $T_P = 1$ s and different amplitudes (a) $A_p = 0.20$ g, (b) $A_p = 0.35$ g, (c) $A_p = 0.55$g for the three distinct values of gravitational multiplier $\alpha = 0.17, 0.38$ and 1.00. Figure 13a shows that the system does not uplift for $\alpha = 1.00$. Additionally, Fig. 12b illustrates that the RB will rock for all gravitational multiplier values but the response for $\alpha = 1.00$ will exhibit the smallest amplitude, with a large difference compared to $\alpha = 0.17$ and 0.38. However, the maximum angular velocity of the RB for $\alpha = 1.00$ is very close to the other two cases. Figure 13c highlights that, interestingly the RB for $\alpha = 1.00$ overturns first, even if it was the last to uplift compared to the other two. This observation is rather counterintuitive, since

(a)

(b)

(c)
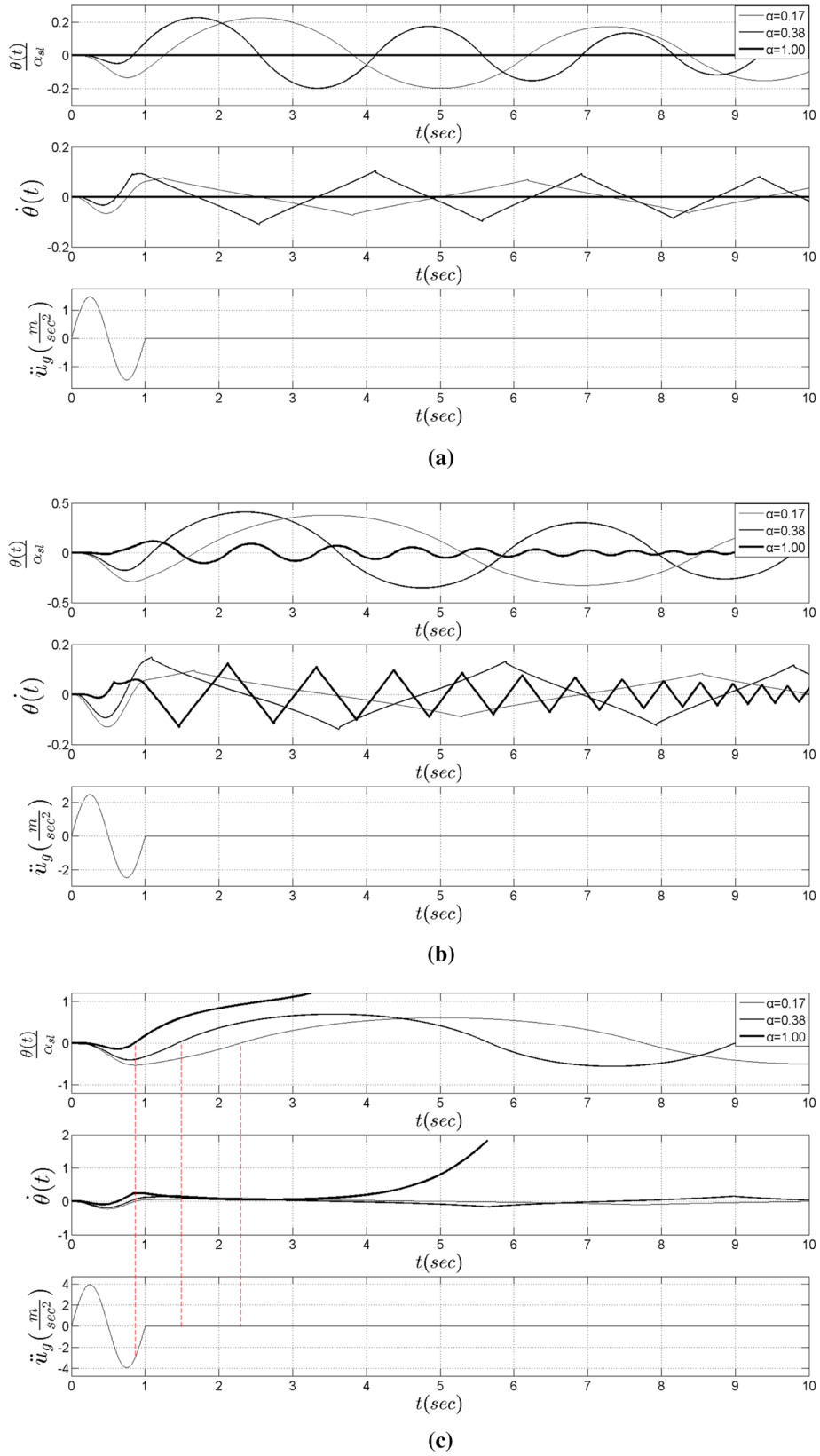
Fig. 13 Rocking response of a RB with $R = 7.21$ and $\alpha_{sl} = 1/4$ when subjected to a single sinusoidal pulse with period $T_P = 1.00$ s, and different amplitudes **a** $A_p = 0.20$ g, **b** $A_p = 0.35$ g, **c** $A_p = 0.55$ g for $\alpha = 0.17, 0.38$ and 1.00
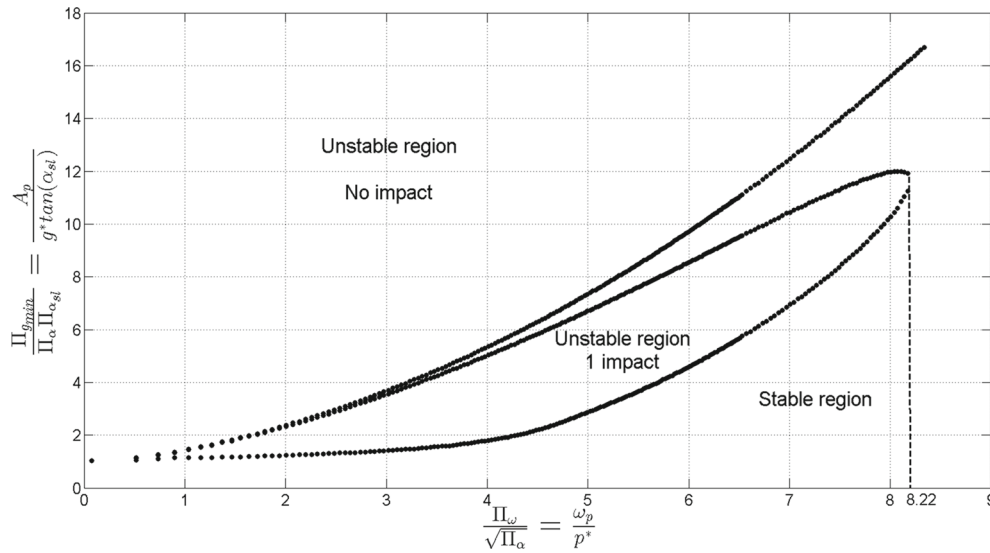
Fig. 14 Self-similar rocking overturning spectrum for a rigid block of $\Pi_{\alpha_{sl}} = 1/4$, subjected to a one-cycle sinusoidal excitation

gravity acts as a stabilizing factor. The reason for this overturning event is that the system for $\alpha = 1.00$ has a bigger p resulting in an impact (zero crossing) at an earlier time for the first rocking cycle, as indicated in the figure. Thus, just after the first impact, the system for $\alpha = 1.00$ receives an extra "push" from the excitation and this proves to be a critical parameter for this case. An additional factor to assist in the overturning is that angular velocities for $\alpha = 1.00$ are higher than the cases of $\alpha = 0.17$ and $\alpha = 0.38$ as mentioned above.

The self-similar behavior of the system is shown in Fig. 14, which presents the overturning spectrum of the RB, $\frac{\Pi_{g_{min}}}{\Pi_\alpha \Pi_{\alpha_{sl}}}$ against $\frac{\Pi_\omega}{\sqrt{\Pi_\alpha}}$ when $\Pi_{\alpha_{sl}} = 1/4$. It has been proven that a freestanding rigid block under sinusoidal pulses may overturn with two distinct modes [10,13,32,33]. The first mode of overturning occurs by exhibiting at least one impact and the second without any impact. However, to deduce the effect of low gravity on the overturning spectrum of the RRB, Fig. 15 plots the minimum overturning acceleration, $\frac{\Pi_{g_{min}}}{\Pi_{\alpha_{sl}}}$, against Π_ω for the three distinct values of Π_α. Overturning without any impact always requires higher values of A_p than overturning with impact for a certain value of Π_α. Moreover, the plot in Fig. 15 can be separated into four characteristic regions (A, B, C and D). Region A is defined for $0 < \Pi_\omega \leq 2.23$ where the first overturning
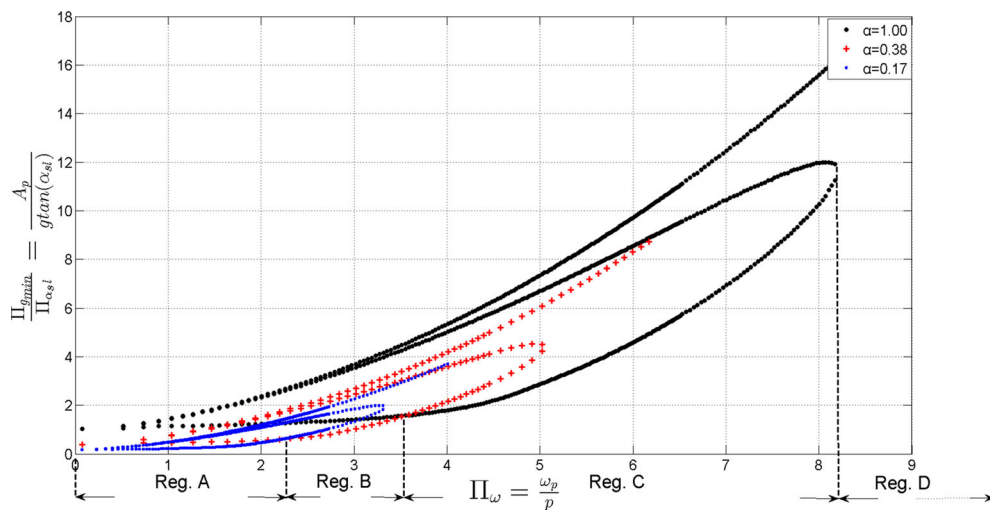
Fig. 15 Rocking overturning spectra of rigid blocks with $\Pi_{\alpha_{sl}} = 1/4$, subjected to one-cycle sinusoidal excitation, concerning the gravitational multipliers $\alpha = 0.17$, 0.38 and 1.00

happens for the RB with $\alpha = 0.17$. Region B is $2.23 < \frac{\omega_p}{p} \leq 3.61$ where the first overturning occurs for $\alpha = 0.38$. Region C corresponds to $3.61 < \frac{\omega_p}{p} \leq 8.22$ with the first overturning occurring for $\alpha = 1.00$. The RB in regions B and C exhibits a counterintuitive behavior since one would expect that the lower gravity leads to an easier overturning for a given value of A_p. Such phenomenon lies above the response illustrated in Figure 13c and has already been explained in this subsection. Finally, region D ($8.22 < \frac{\omega_p}{p}$) is the safest, as one can observe only overturning without impact that corresponds firstly to $\alpha = 0.17$, then to $\alpha = 0.38$ and finally to $\alpha = 1.00$ which is the expected behavior of the RB, since gravity acts as a stabilizing factor.
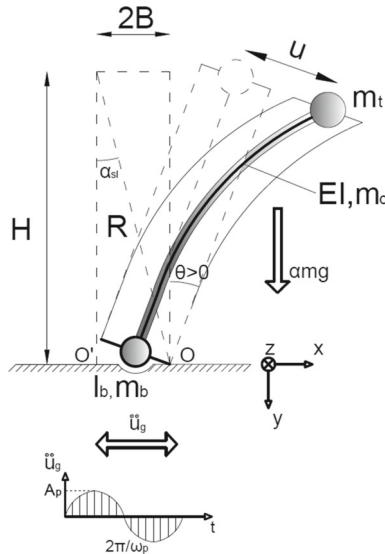
2.5 Flexural rocking block (FRB)

The rigid block model in some earthquake engineering applications can be characterized as unrealistic and incompatible with the structures that display flexural characteristics. Hence, in this subsection, the block is simulated as a deformable rocking column characterized by a uniformly distributed mass (m_c) and stiffness (EI) as shown in Fig. 16. Several authors in the past have considered similar models [21,31,34]. However, Vassiliou et al. [31] investigated the analytical formulation in depth and proposed the model used in this study. The total mass of the column (m_c) is also uniformly distributed along the height. Two additional lumped masses are located at the top (m_t) and base (m_b), while the moment of inertia (I_b) is considered around the center of mass. The width of the base is defined as $2B$. Similarly to rigid blocks, the slenderness is: $a_{sl} = a \tan\left(\frac{B}{H}\right)$, and the surface is assumed to be rigid. The flexural block subjected to rocking is a dynamic system of two degrees of freedom (DOFs). The first DOF is the base rotation (θ) and the second one is the horizontal displacement of the top with respect to the bottom of the column (u).

When there is no uplift the motion is described by the same equation as this of a flexural vertical cantilever fixed to the base.

$$\ddot{u} + 2\xi\omega_n\dot{u} + \omega_n^2 u = -\tilde{\Gamma}\ddot{u}_g \tag{21}$$

where ξ: represents the damping ratio associated with the energy dissipated during the vibration of the column (viscous classical damping), $\omega_n = \frac{\tilde{k}}{\tilde{m}}$, $\tilde{m} = m_t + \frac{33}{140}m_c$: expresses the generalized mass, $\tilde{k} = 3\frac{EI}{H^3}$: represents the generalized stiffness and $-\tilde{\Gamma}\ddot{u}_g = -\frac{m_t + \frac{3}{8}m_c}{m_t + \frac{33}{140}m_c}\ddot{u}_g$ is equal to the excitation of the system.

Fig. 16 Flexural rocking block model

When the system uplifts, the rocking behavior is described by two DOFs (θ, u). By applying the Lagrangian formulation (see [31]), one can produce the equations of motion shown in Eqs. (22) and (23).

$$\left(I_{\mathrm{b}} + m_{\mathrm{c}}\left(B^2 + \frac{H^2}{3}\right) + \frac{33}{140}m_{\mathrm{c}}u^2 - sign\theta\frac{3}{4}Bum_{\mathrm{c}} + m_{\mathrm{t}}\left(B^2 + H^2\right) - sign\theta 2Bum_{\mathrm{t}} + m_{\mathrm{t}}u^2\right)\ddot{\theta}$$

$$= -\left(\frac{33}{70}m_{\mathrm{c}} + 2m_{\mathrm{t}}\right)u\dot{u}\dot{\theta} - \left(\frac{11}{40}m_{\mathrm{c}} + m_{\mathrm{t}}\right)H\ddot{u} + sign\theta\left(\frac{3}{4}m_{\mathrm{c}} + 2m_{\mathrm{t}}\right)B\dot{u}\dot{\theta}$$

$$+ \left(-sign\theta\left(m_{\mathrm{t}} + m_{\mathrm{c}} + m_{\mathrm{b}}\right)B\sin\theta - \left(\frac{m_{\mathrm{c}}}{2} + m_{\mathrm{t}}\right)H\cos\theta + \left(\frac{3}{8}m_{\mathrm{c}} + m_{\mathrm{t}}\right)u\sin\theta\right)\ddot{u}_g$$

$$+ \left(-sign\theta\left(m_{\mathrm{t}} + m_{\mathrm{c}} + m_{\mathrm{b}}\right)B\cos\theta - \left(\frac{m_{\mathrm{c}}}{2} + m_{\mathrm{t}}\right)H\sin\theta + \left(\frac{3}{8}m_{\mathrm{c}} + m_{\mathrm{t}}\right)u\cos\theta\right)(\alpha g) \quad (22)$$

$$\left(\frac{33}{140}m_{\mathrm{c}} + m_{\mathrm{t}}\right)\ddot{u} + \left(\frac{11}{40}m_{\mathrm{c}} + m_{\mathrm{t}}\right)H\ddot{\theta}$$

$$= -3\frac{\mathrm{EI}}{H^3}u - c\dot{u} + \left(\frac{3}{8}m_{\mathrm{c}} + m_{\mathrm{t}}\right)(\alpha g)\sin\theta$$

$$+ \left(\left(\frac{33}{140}m_{\mathrm{c}} + m_{\mathrm{t}}\right)u - sign\theta\left(\frac{3}{8}m_{\mathrm{c}} + m_{\mathrm{t}}\right)B\right)\dot{\theta}^2 - \left(\frac{3}{8}m_{\mathrm{c}} + m_{\mathrm{t}}\right)\ddot{u}_g\cos\theta \quad (23)$$

The uplift condition of the system is a function [Eq. (26)] of the overturning (M_{ot}) and restoring (M_{rt}) moments about a pivot point (Fig. 16). More specifically,

$$M_{\mathrm{ot}} = -\ddot{u}H\left(m_{\mathrm{t}} + \frac{11}{40}m_{\mathrm{c}}\right) - \left(m_{\mathrm{t}} + \frac{m_{\mathrm{c}}}{2}\right)\ddot{u}_g H; \quad (24)$$

$$M_{\mathrm{rt}} = (m_{\mathrm{b}} + m_{\mathrm{c}} + m_{\mathrm{t}})(ag)B \pm \left(\frac{3}{8}m_{\mathrm{c}} + m_{\mathrm{t}}\right)(\alpha g)u \quad (25)$$

where the upper and the lower signs denote moments about the right and the left pivot point, respectively. By combining Eqs. (24) and (25), the uplift condition which is described in Eq. (26) is defined.

$$\pm(M_{\mathrm{ot}} + M_{\mathrm{rt}}) > 0 \Leftrightarrow$$

$$\pm H\left(m_{\mathrm{t}} + \frac{11}{40}m_{\mathrm{c}}\right)\left(\omega_n^2 u + 2\xi\omega_n\ddot{u} + \tilde{\Gamma}\ddot{u}_g\right) \mp \left(m_{\mathrm{t}} + \frac{m_{\mathrm{c}}}{2}\right)\ddot{u}_g H$$

$$- (m_{\mathrm{b}} + m_{\mathrm{c}} + m_{\mathrm{t}})(ag)B \pm \left(\frac{3}{8}m_{\mathrm{c}} + m_{\mathrm{t}}\right)(\alpha g)u > 0. \quad (26)$$

The modeling of the dissipated energy at impact during the rocking of a deformable block constitutes a field of interest for many researchers [18,21,31]. The approach of Acikgoz and Dejong (ADJex) [21] is adopted herein and considers two possible states after the impact. In the first state, after the impact the block's base stays on the ground and experiences a full contact phase, while in the second state, the block immediately uplifts about the opposite corner and continues to rock. The 'decision' between these two possible states is taken by considering the minimum of the total energy of the rocking system under the restriction that the amount of the post-impact kinetic energy must be less than the pre-impact kinetic energy. Acikgoz and Dejong enforce energy decrease through the conservation of the horizontal momentum instead of that of angular momentum, which in certain cases leads to energy increase after impact.

In the full contact phase:

$$\dot{u}_2 = \frac{\left(I_{\mathrm{bc}} - 2m_{\mathrm{b}}B^2 + m_{\mathrm{c}}\left(-B^2 + \frac{H^2}{3} + \frac{33}{140}u^2\right) + m_{\mathrm{t}}\left(-B^2 + H^2 + u^2\right)\right)}{\left(\frac{11}{40}m_{\mathrm{c}} + m_{\mathrm{t}}\right)H}\dot{\theta} + \dot{u} \quad (27)$$

The indicies '1' and '2' denote the pre- and the post-impact states of the system.

$$E_{2,fc} = \frac{1}{2}\left(m_{\mathrm{t}} + \frac{33}{140}m_{\mathrm{c}}\right)\dot{u}_2^2 \quad (28)$$

Due to the instantaneous character of the impact, $u_2 = u_1$ and $\theta_2 = \dot{\theta}_2 = 0$.

In the immediate rocking phase:

There are two unknown quantities. The first is the post-impact angular velocity of the base ($\dot{\theta}_2$) and the second is the post-impact relative horizontal velocity of the top mass (m_t) with respect to the base of the block ($\dot{u}_2$). As mentioned above, in order to conserve the horizontal momentum, Acikgoz and Dejong [21] made the assumption that the relative horizontal velocity remains the same after impact, that is: $\dot{u}_2 = \dot{u}_1$.

Hence, by adopting the above assumption and applying the conservation of angular momentum around an impact corner, one can derive the following equations:

$$\dot{\theta}_2 = \frac{(I_{bc} - 2B^2 m_b) + m_c \left(-B^2 + \frac{H^2}{3} + \frac{33}{140}u_1^2\right) + m_t \left(-B^2 + H^2 + u_1^2\right)}{I_{bc} + m_c \left(B^2 + \frac{H^2}{3} + \frac{33}{140}u_1^2 \pm \frac{3}{4}Bu_1\right) + m_t \left(B^2 + H^2 + u_1^2 \pm 2Bu_1\right)} \dot{\theta}_1 \tag{29}$$

where the upper sign corresponds to impact on the left corner and the lower sign corresponds to the right corner of the block.

The kinetic energy is given by the following equation:

$$E_{2,r} = \frac{1}{2}I_{bc}\dot{\theta}^2 + \frac{1}{2}m_c \left(\left(B^2 + \frac{H^2}{3} + \frac{33}{140}u^2 \pm \frac{3}{4}Bu\right)\dot{\theta}_2^2 + \frac{33}{140}\dot{u}_2^2 + \frac{11}{20}H\dot{\theta}_2\dot{u}_2\right)$$
$$+ \frac{1}{2}m_t \left((B^2 + H^2 + u^2 \pm 2Bu)\dot{\theta}_2^2 + \dot{u}_2^2 + 2H\dot{\theta}_2\dot{u}_2\right) \tag{30}$$

following the sign convention of Eq. (25)

If E_1 is the prior to the impact kinetic energy of the system, in case $(E_r, E_{fc}) > E_1$, then the conservation of horizontal momentum leads to:

$$\dot{u}_2 = \frac{\left(\frac{m_c}{2} + m_t\right)H}{\frac{3}{8}m_c + m_t}\dot{\theta}_1 + \dot{u}_1 \tag{31}$$

The response is a function of 13 variables:

$$(u, \theta) = f\left(\omega_n, m, m_c, m_b, I_b, \xi, \alpha_{sl}, p, g, \omega_p, A_p, a\right) \tag{32}$$

Through the application of dimensional analysis, the response can be described by $14 - 3 = 11$ dimensionless parameters:

$$\Pi_\theta = \frac{\theta}{\theta_{cr}}; \; \Pi_u = \frac{u}{u_{cr}}; \; \Pi_{\alpha_{sl}} = \tan(\alpha_{sl}); \; \Pi_\alpha = \alpha$$

$$\Pi_g = \frac{A_p}{g}; \; \Pi_{\omega_p} = \frac{\omega_p}{p}; \; \Pi_{\omega_n} = \frac{\omega_n}{p}; \; \Pi_\xi = \xi$$

$$\Pi_{m_c} = \gamma_{mc} = \frac{m_c}{m}; \; \Pi_{mb} = \gamma_{mb} = \frac{m_b}{m}; \; \Pi_{I_b} = \gamma_{Ib} = \frac{I_b}{\frac{4}{3}m_b B^2} \tag{33}$$

And the response can be expressed as

$$\left(\frac{u}{u_{cr}}, \frac{\theta}{\theta_{cr}}\right) = f\left(\frac{\omega_n}{p}, \frac{\omega_p}{p}, \gamma_{mc}, \gamma_{mb}, \gamma_{Ib}, \xi, \alpha, \frac{A_p}{g \tan a_{sl}}\right) \tag{34}$$

where

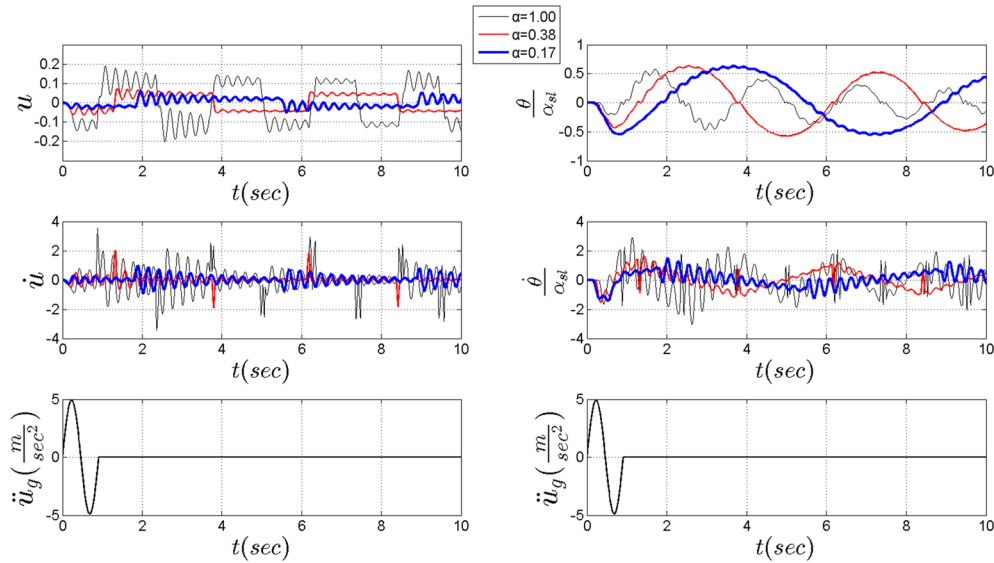$$\omega_n = \sqrt{\frac{\frac{3EI}{H^3}}{\left(m_t + \frac{33}{140}m_c\right)}} \tag{35}$$

$$p = \sqrt{\frac{g}{R}} \tag{36}$$

$$\gamma_{mc} = \frac{m_c}{m_t}, \quad \gamma_{mb} = \frac{m_b}{m_t}, \quad \gamma_{Ib} = \left(\frac{I_b}{\frac{4}{3}m_b B^2}\right) \tag{37}$$

$$\theta_{\text{cr}} = \tan^{-1}\left(\frac{m_{\text{t}} + m_{\text{b}} + m_{\text{c}}}{m_{\text{t}} + \frac{m_{\text{c}}}{2}}\frac{B}{H}\right) \tag{38}$$

$$u_{\text{cr}} = \frac{(m_{\text{t}} + m_{\text{b}} + m_{\text{c}})\,Bg}{\left(m_{\text{t}} + \frac{11}{40}m_{\text{c}}\right)H\omega_n^2 + \left(\frac{3}{8}m_{\text{c}} + m_{\text{t}}\right)g} \tag{39}$$

Figures 17 and 18 present the rocking response of the flexural block with $\frac{\omega_n}{p} = 5$ and $\frac{\omega_n}{p} = 20$, respectively for $\gamma_{\text{mb}} = 2, \gamma_{\text{mc}} = 1, \frac{\omega_p}{p} = 7, \frac{A_p}{g\tan(\alpha_{\text{sl}})} = 5, \alpha_{\text{sl}} = 0.1$ and for the three distinct values of gravitational multiplier, $a = 0.17, 0.38, 1.00$.

Fig. 17 Rocking response of a flexural block when subjected to a sinusoidal pulse for $\alpha = \{1.00, 0.38, 0.17\}$ where: $\frac{\omega_n}{p} = 5$, $\gamma_{\text{mb}} = 2, \gamma_{\text{mc}} = 1, \frac{\omega_p}{p} = 7, \frac{A_p}{g\tan(a_{\text{sl}})} = 5, \alpha_{\text{sl}} = 0.1$
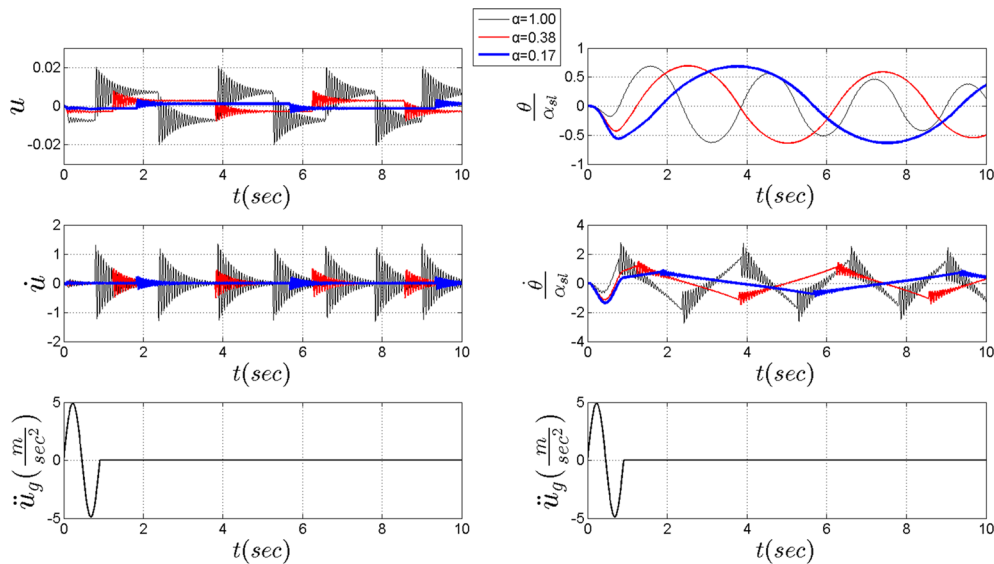
Fig. 18 Rocking response of a flexural block when subjected to a sinusoidal pulse for $\alpha = \{1.00, 0.38, 0.17\}$ where: $\frac{\omega_n}{p} = 20$, $\gamma_{\text{mb}} = 2, \gamma_{\text{mc}} = 1, \frac{\omega_p}{p} = 7, \frac{A_p}{g\tan(a_{\text{sl}})} = 5, \alpha_{\text{sl}} = 0.1$
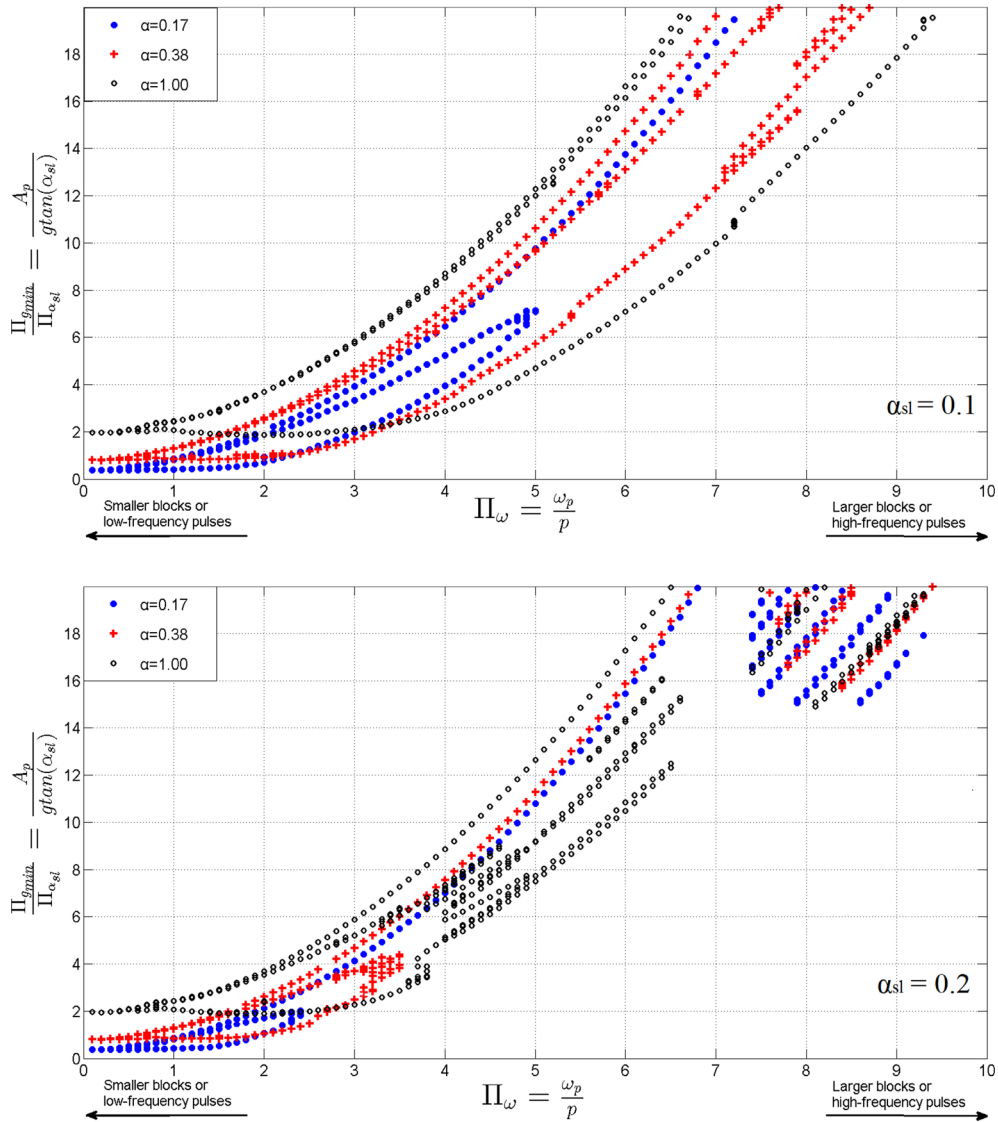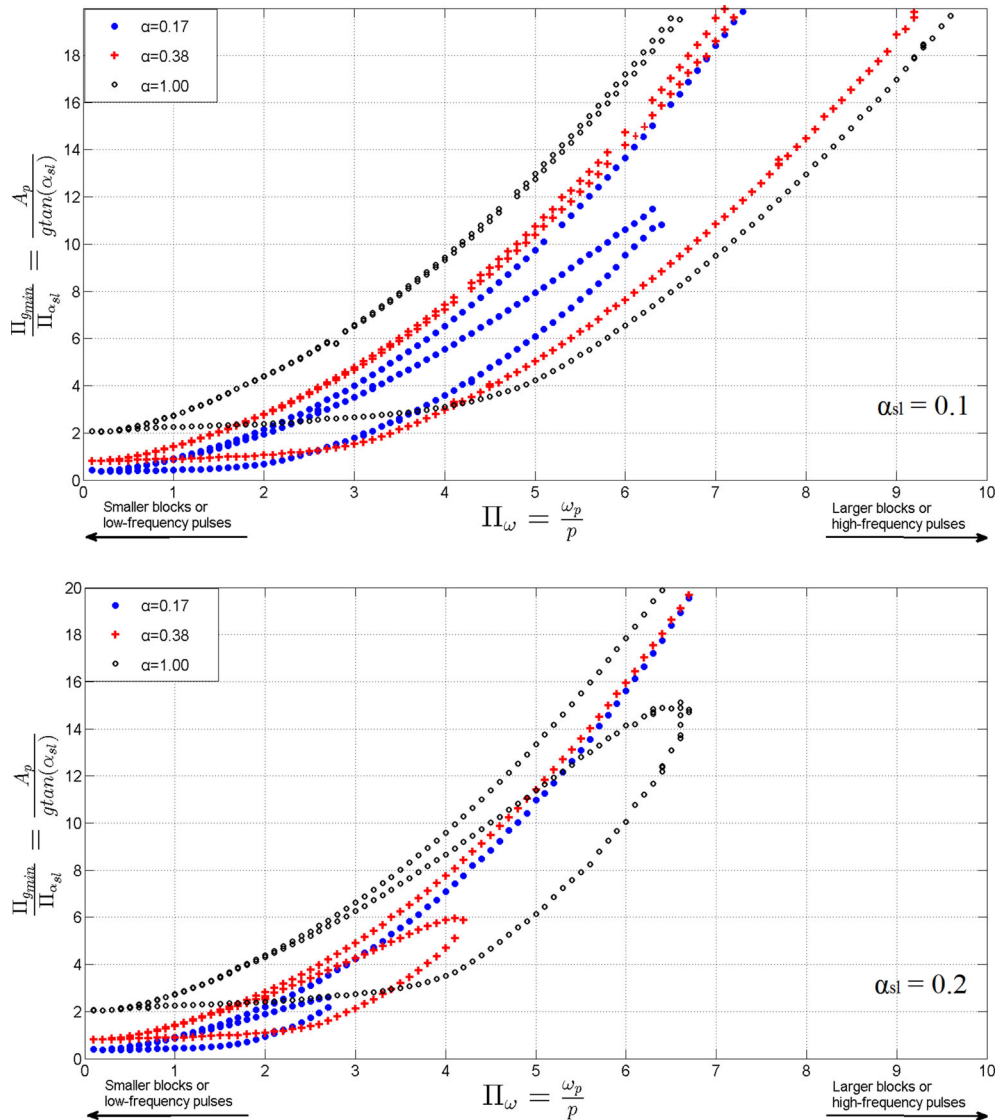
Fig. 19 Rocking spectra of a flexural block when subjected to a sinusoidal pulse for $\alpha = \{1.00, 0.38, 0.17\}$ where: $\frac{\omega_n}{p} = 5$, $\gamma_{mb} = 1$, $\gamma_{mc} = 1$

The RRB system analysis has shown that generally low gravity does not act beneficially for rocking (except for regions B and C in Fig. 15—for a single sinusoidal pulse), but on the other hand, Fig. 11 illustrates the beneficial effect of low gravity on the vertical cantilever system. In this case, the FRB system couples the two systems together. From Figs. 17 and 18, it can be deduced that low gravity significantly lengthens the rocking cycles through the "rocking frequency" (p) but it is very beneficial regarding the flexural response, Π_u, as this decreases significantly in accordance with Fig. 11. The latter observation is also a result of the stronger gravitational field when $\alpha = 1.00$, which leads to higher angular velocities prior and post-impact, compared to the $\alpha = 0.17$ and 0.38 cases. The higher post-impact angular velocities for $\alpha = 1.00$ amplify the flexural response accordingly, independent of other parameters, such as Π_{ω_n} or Π_ξ. Lower values of Π_{ω_n} combined with higher gravitational multipliers (Fig. 17- blue thick line), lead to flexible FRB which is affected more by the $p - \Delta$ effects (due to the higher gravity). The jaggedness of the θ / α_{sl} curve for $\alpha = 1.00$ in Fig. 17 confirms the aforementioned observation.

Fig. 20 Rocking spectra of a flexural block when subjected to a sinusoidal pulse for $\alpha = \{1.00, 0.38, 0.17\}$ where: $\frac{\omega_n}{p} = 20$, $\gamma_{mb} = 1$, $\gamma_{mc} = 1$

The FRB is a complex system affected by many dimensionless parameters as shown in Eqs. (32) and (33). This study chooses to present only the most important aspects of its response. Four representative overturning spectra of FRB subjected to a single sinusoidal impulse are shown in Figs. 19 and 20, for different values of dimensionless stiffness $\left(\frac{\omega_n}{p} = \{5, 20\} \right)$, slenderness ($\alpha_{sl} = 0.1, 0.2$), and gravitational multiplier ($\alpha = 0.17, 0, 38$ and 1.00). As in the case of the RRB, the sequence concerning regions A, B and C is the same for each spectrum. However, region C dominates the range ω_p/p, and hence, low gravity plays a more beneficial role than expected, especially for large blocks or high-frequency pulses ($\frac{\omega_p}{p} > 3 - 4$). On the contrary, region D cannot be defined, since it varies for different values of the aforementioned parameters. Slenderness (α_{sl}) is important when it comes to overturning of a block, since for $\alpha_{sl} = 0.1$ we observe a broadened area of mode-1 overturning (with one impact), while for $\alpha_{sl} = 0.2$ this area is substantially limited. On the other hand, the area of overturning without impact is slightly different from spectrum to spectrum, irrespective of the stiffness and slenderness of the flexural block, or of the gravitational conditions.

Table 1 Comparison of the dynamic characteristics of the under study fundamental dynamic systems (*SP, RIP, FIP, RRB, FRB*)

Parameters/characteristics	Simple pendulum (SP)	Rigid inverted pendulum (RIP)	Flexural inverted pendulum (FIP)	Rigid rocking block (RRB)	Flexural rocking block (FRB)
Restoring mechanism	Gravity	Elasticity (rotational spring)	Elasticity (rotational spring and structure)	Gravity ($\theta < \alpha_{sl}$)	Gravity and counteracting elasticity, ($\theta < \alpha_{sl}$)
Destabilizing mechanism	External imposed conditions	Gravity	Gravity, $p - \Delta$ effects	External imposed conditions, gravity ($\theta > \alpha_{sl}$)	Gravity and elasticity, ($\theta > \alpha_{sl}$)
Restoring force/moment	$F_r = -m\alpha g \sin\theta$	$M_r = K_r\theta$	$M_r = K_r\theta \quad F_r = KLu$	$M_r = -m\alpha g R \sin(\pm\alpha_{sl} - \theta)$	$M_r = -\left(\frac{11}{40}m_c + m_t\right) H\dot{u}\, F_r$ $= -\left(\frac{11}{40}m_c + m_t\right) H\dot{\theta} - Ku$
Frequency parameter	$\omega_{0,sp} = \sqrt{\frac{\alpha g}{L}}$	$\omega_{0,RIP} = \sqrt{\frac{K_r}{mL^2} - \alpha\frac{g}{L}}$	$\omega_{0,FIP} =$ $\sqrt{\frac{K_r k - m\alpha g Lk - m^2\alpha^2 g^2}{K_r m + mL^2 k + m^2\alpha g L}}$	$p_{RRB} = \sqrt{\frac{3\alpha g}{4R}}$	$p_{FRB} = \sqrt{\frac{\alpha g}{R}}$ Before uplift: $\omega_n = \sqrt{\frac{\frac{3EI}{H^3}}{\left(m_t + \frac{33}{140}m_c\right)}}$ After uplift: $\omega_{up,2} = \lambda\omega_n$
Low gravity effect	Negative	Positive	Positive	Depends on $\left\{\frac{\omega_p}{p}, \alpha_{sl}\right\}$ (see Fig. 15)	Depends on $\left\{\frac{\omega_p}{p}, \frac{\omega_n}{p}, \alpha_{sl}\right\}$ (see Figs. 19, 20)
Prerequisite for the motion	$0 < \alpha$	$0 < \alpha < \alpha_{cr}$	$0 < \alpha < \alpha'_{cr}$	$0 < \alpha < \frac{A_p}{g\tan(\alpha_{sl})}$	$\pm (M_{ot} + M_{rt}) > 0$ [see Eq. (26)]
Dimensionless parameters	$\Pi_\theta, \Pi_\alpha, \Pi_g, \Pi_{T_{SP}}$	$\Pi_\theta, \Pi_\alpha, \Pi_g,$ $\Pi_{\alpha_{cr}}, \Pi_{T_{RIP}}$	$\Pi_\theta, \Pi_\alpha, \Pi_g, \Pi_{\alpha_{cr}},$ Π_k or $\Pi_{k_{cant}}, \Pi_{T_{FIP}}$	$\Pi_\theta, \Pi_\omega, \Pi_{\alpha_{sl}}, \Pi_\alpha, \Pi_g$	$\Pi_\theta, \Pi_u, \Pi_{\alpha_{sl}},$ $\Pi_\alpha, \Pi_g, \Pi_{\omega_p}, \Pi_{\omega_n},$ $\Pi_\xi, \Pi_{m_c}, \Pi_{m_b}, \Pi_{I_b}$

3 Conclusions

This paper revisits the fundamental structural dynamic systems to investigate the effect of low gravity on their dynamic characteristics and their response when subjected to a sine pulse. It begins by using dimensional analysis for the formulation of positive stiffness vibration models, such as the simple pendulum (SP), the rigid inverted pendulum (RIP), and the flexural inverted pendulum (FIP), and concludes with (negative stiffness) rocking system models: the rigid rocking block (RRB) and the flexural rocking block (FRB). The sine pulse was chosen as the simplest harmonic excitation and in order to reveal any critical trends or patterns regarding the effect of low gravity.

The conclusions of this study can be summarized as follows:

- The SP—studied here purely as a reference case—becomes a more flexible configuration as the gravitational multiplier decreases (low gravity). This results in an amplification of the response in the vicinity of the resonant frequency. On the other hand, this increase in flexibility occurs for a wider range of $T_{0,SP}/T_p$, indicating less sensitivity to the frequency content of the excitation. The response is self-similar and can be described by a master curve as shown in Fig. 2.
- The change in gravity has exactly the opposite effect on the RIP. Low gravity forms a stiffer RIP config-uration and thus decreases the response accordingly. The response in this case is also self-similar and can be described by the master curve in Fig. 6. The beneficial effect of low gravity is further highlighted in Fig. 7.
- The FIP, the last of the vibrating systems, is also the most complex, as it combines a rotational with a translational/flexural DOF in series, resembling a Maxwell element. This system is a pseudo-SDOF, as no mass is assigned to the rotational DOF. By considering $k = 3\frac{EI}{L^3} - \frac{\alpha mg}{L}$ and $\alpha'_{cr} = a_{cr}\left(\frac{k_{cant}L^2}{K_r + k_{cant}L^2}\right)$ in order to take $p - \Delta$ effects into account, the system exhibits a self-similar behavior similar to the RIP. Interestingly, we find that although the RIP and the vertical cantilever appear to be two different systems, they are actually two aspects of the FIP; as such, we prove that they exhibit the same dimensionless response, defined by the master curve of Fig. 10. The beneficial role of low gravity is shown in Fig. 11.
- The RRB is the simplest rocking model and is affected by low gravity in three ways: (a) the uplift of the block occurs for lower excitation amplitudes (A_p); (b) the "rocking frequency" parameter, p, results in longer rocking cycles; and (c) weakening of the gravitational field results in lower angular velocities. However, the effect is not the same over the entire range of ω_p/p values; in regions A and D, low gravity acts detrimentally (as expected), while in regions B and C, it acts beneficially, as explained in Fig. 13.
- The FRB is a complex system that combines rocking with flexural response. Because gravity acts as a stabilizing force in rocking, but in most cases as a destabilizing force in vibrations, this introduces an added complexity. The effect of low gravity with respect to the rocking response is -similar to that of the RRB-, divided into three regions A, B and C (Figs. 19 and 20), with no reliable/discernible region D. Nevertheless, when flexure is more dominant in the system $\left(\frac{\omega_n}{p} = 5\right)$, low gravity plays a beneficial role for larger blocks, where $\frac{\omega_p}{p} > 3 - 3.5$.

Table 1 summarizes all key results of this study for the 5 main systems analyzed, comparing and contrasting the stabilizing and destabilizing factors, frequency parameters and gravity effects.

This study has revisited the main structural systems from an extraterrestrial civil engineering point of view. Although such applications are not yet underway, this study anticipates them based on the enormous streamline of investments that have taken place in recent years by world-leading firms and federal agencies (NASA, SpaceX, Boeing, Virgin Galactic, ESA). These investments will most assuredly require the extension of civil engineering in extraterrestrial conditions, be it for the development of Lunar and Martian outposts or for Space tourism.

where

$$\lambda = \sqrt{\frac{I_{bc} + m_c\left(\frac{H^2}{3} + B^2\right) + m_t\left(H^2 + B^2\right)}{I_{bc} + m_c\left(\frac{H^2}{3} + B^2\right) + m_t\left(H^2 + B^2\right) - \frac{\left(\frac{11}{40}m_c + m_t\right)^2 H^2}{\frac{11}{40}m_c + m_t}}}$$

Appendix

Derivation of the equations of motion [Eqs. (9) and (10)] of the FIP dynamic system.
The kinetic energy of the FIP dynamic system is equal to:

$$T = \frac{1}{2}m \left(\dot{u}_g^2 + 2\dot{u}_g L \cos\theta\,\dot{\theta} - 2\dot{u}_g u \sin\theta\,\dot{\theta} + 2\dot{u}_g \dot{u} \cos\theta + L^2\dot{\theta}^2 + u^2\dot{\theta}^2 + \dot{u}^2 + 2L\dot{\theta}\dot{u} \right) \tag{A1}$$

The potential energy of the FIP dynamic system due to gravity, D'Alembert forces and strain energy is equal to:

$$V = \frac{1}{2}K_r\theta^2 + \frac{3}{2}\frac{\mathrm{EI}}{L^3}u^2 - m\,(\alpha g)\,(L\,(1-\cos\theta) + u\sin\theta) \tag{A2}$$

Lagrange equations:

$$\frac{\mathrm{d}}{\mathrm{d}t}\frac{\partial\,(T-V)}{\partial\dot{\theta}} - \frac{\partial\,(T-V)}{\partial\theta} = 0 \tag{A3}$$

$$\frac{\mathrm{d}}{\mathrm{d}t}\frac{\partial\,(T-V)}{\partial\dot{u}} - \frac{\partial\,(T-V)}{\partial u} = -c\dot{u} \tag{A4}$$

References

1. Chopra, A.K.: Dynamics of Structures: Theory and Applications to Earthquake Engineering. Prentice Hall, Englewood Cliffs (2007)
2. Clough, R.W., Penzien, J.: Dynamics of Structures. McGraw-Hill, New York (2013)
3. Mylonakis, G., Gazetas, G.: Seismic soil–structure interaction: beneficial or detrimental? J. Earthq. Eng. **4**, 277–301 (2000)
4. Avilés, J., Pérez-Rocha, L.E.: Soil–structure interaction in yielding systems. Earthq. Eng. Struct. Dyn. **32**, 1749–1771 (2003)
5. Mylonakis, G., Syngros, C., Gazetas, G., Tazoh, T.: The role of soil in the collapse of 18 piers of Hanshin expressway in the Kobe earthquake. Earthq. Eng. Struct. Dyn. **35**, 547–575 (2006)
6. Gazetas, G., Anastasopoulos, I., Gerolymos, N., Mylonakis, G., Syngros, C.: The collapse of the Hanshin expressway (Fukae) Bridge, Kobe 1995: soil-foundation-structure interaction, reconstruction, seismic isolation. In: Entwicklungen in der Bodenmechanik, Bodendynamik und Geotechnik: Festschrift zum 60. Geburtstag von Univ.-Professor Dr.-Ing. habil. Stavros A. Savidis. pp. 93–120 (2006)
7. European Commitee for Standardization: Eurocode 8: design of structures for earthquake resistance—Part 1: general rules, seismic actions and rules for buildings, vol 1, p 231 . European Commitee for Standardization (2004)
8. Kirkpatrick, P.: Seismic measurements by the overthrow of columns. Bull. Seismol. Soc. Am. **17**, 95–109 (1927)
9. Housner, G.W.: The behavior of inverted pendulum structures during earthquakes. Bull. Seismol. Soc. Am. **53**, 403–417 (1963)
10. Zhang, J., Makris, N.: Rocking response of free-standing blocks under cycloidal p. J. Eng. Mech. **127**, 473–483 (2001)
11. Makris, N., Konstantinidis, D.: The rocking spectrum and the limitations of practical design methodologies. Earthq. Eng. Struct. Dyn. **32**, 265–289 (2003)
12. Makris, N., Vassiliou, M.F.: Planar rocking response and stability analysis of an array of free-standing columns capped with a freely supported rigid beam. Earthq. Eng. Struct. Dyn. **42**, 431–449 (2013)
13. Makris, N., Kampas, G.: Size versus slenderness: two competing parameters in the seismic stability of free-standing rocking columns. Bull. Seismol. Soc. Am. **106**, 104–122 (2016)
14. Apostolou, M., Gazetas, G., Garini, E.: Seismic response of slender rigid structures with foundation uplifting. Soil Dyn. Earthq. Eng. **27**, 642–654 (2007)
15. Gelagoti, F., Kourkoulis, R., Anastasopoulos, I., Gazetas, G.: Rocking-isolated frame structures: margins of safety against toppling collapse and simplified design approach. Soil Dyn. Earthq. Eng. **32**, 87–102 (2012)
16. Antonellis, G., Panagiotou, M.: Seismic response of bridges with rocking foundations compared to fixed-base bridges at a near-fault site. J. Bridge Eng. **19**, 04014007 (2014)
17. Freddi, F., Dimopoulos, C.A., Karavasilis, T.L.: Rocking damage-free steel column base with friction devices: design procedure and numerical evaluation. Earthq. Eng. Struct. Dyn. **46**, 2281–2300 (2017)
18. Oliveto, G., Calio, I., Greco, A.: Large displacement behaviour of a structural model with foundation uplift under impulsive and earthquake excitations. Earthq. Eng. Struct. Dyn. **32**, 369–393 (2003)

19. Psycharis, I.N., Jennings, P.C.: Rocking of slender rigid bodies allowed to uplift. Earthq. Eng. Struct. Dyn. **11**, 57–76 (1983)
20. Chopra, A.K., Yim, S.C.-S.: Simplified earthquake analysis of structures with foundation uplift. J. Struct. Eng. **111**, 906–930 (1985)
21. Acikgoz, S., Dejong, M.J.: The interaction of elasticity and rocking in flexible structures allowed to uplift. Earthq. Eng. Struct. Dyn. **41**, 2177–2194 (2012)
22. Vassiliou, M.F., Makris, N.: Analysis of the rocking response of rigid blocks standing free on a seismically isolated base. Earthq. Eng. Struct. Dyn. **41**, 177–196 (2012)
23. Kwak, H.G., Kim, J.K.: P-Δ effect of slender RC columns under seismic load. Eng. Struct. **29**, 3121–3133 (2007)
24. Faramarz, K., Mehdi, S., Farzane, P.: P-delta effects on earthquake response of structures with foundation uplift. Soil Dyn. Earthq. Eng. **34**, 25–36 (2012)
25. Cesaretti, G., Dini, E., De Kestelier, X., Colla, V., Pambaguian, L.: Building components for an outpost on the Lunar soil by means of a novel 3D printing technology. Acta Astronaut. **93**, 430–450 (2014)
26. Ruess, F., Schaenzlin, J., Benaroya, H.: Structural design of a lunar habitat. J. Aerosp. Eng. **19**, 133–157 (2006)
27. Mottaghi, S., Benaroya, H.: Design of a lunar surface structure. I: design configuration and thermal analysis. J. Aerosp. Eng. **28**, 04014052 (2015)
28. Mottaghi, S., Benaroya, H.: Design of a lunar surface structure. II: seismic structural analysis. J. Aerosp. Eng. **28**, 04014053 (2015)
29. Malla, R.B., Chaudhuri, D.: Dynamic analysis of a 3-D frame-membrane lunar structure subjected to impact. Proc., Earth Space 2008 Conf., ASCE, Reston, VA, 1–10 (2008)
30. Wilkinson, S., Musil, J., Dierckx, J., Gallou, I., de Kestelier, X.: Concept design of an outpost for mars using autonomous additive swarm construction. Acta Futura. **10**, 121–129 (2016)
31. Vassiliou, M.F., Truniger, R., Stojadinović, B.: An analytical model of a deformable cantilever structure rocking on a rigid surface: development and verification. Earthq. Eng. Struct. Dyn. **44**, 2775–2794 (2015)
32. Makris, N, Roussos, Y.: Rocking response and overturning of equipment under horizontal pulse-type motions. Report No. 5, Pacific Earthquake Engineering Research Center, PEER, (1998)
33. Makris, N., Vassiliou, M.F.: Are some top-heavy structures more stable? J. Struct. Eng. **140**, 06014001 (2014)
34. Acikgoz, S., DeJong, M.J.: Analytical modelling of multi-mass flexible rocking structures. Earthq. Eng. Struct. Dyn. **45**, 2103–2122 (2016)